Core and edge-specific functionalisation of graphene quantum dots to improve amino acid sensing and metal sensing.

A thesis submitted towards partial fulfilment of the requirements for the degree of:

Master of Technology in Nano Science and Technology

Submitted by:

Tanay Toppo

Roll no. : M4NST22016

Registration no. : 136366 of 2016-17

Under the supervision of

Prof.(Dr.) Sourav Sarkar

School of Materials Science and Nanotechnology

Jadavpur University
Kolkata – 700032

Course Affiliated to:

Faculty of Interdisciplinary Studies, Law and Management

Jadavpur University
Kolkata, India

2022

M.Tech (Nano Science and Technology)
Course affiliated to:
Faculty of Interdisciplinary Studies,
Law and Management
Jadavpur University
Kolkata, India

CERTIFICATE OF RECOMMENDATION

This is in order to certify that the thesis entitled "Core and edge specific functionalisation of graphene quantum dots to improve amino acid sensing" is a legitimate work done by Tanay Toppo under our supervision and guidance for the purposes of fulfilling the requirement for the degree of Master of Technology in Nano Science and Nanotechnology in the School of Materials Science and Nanotechnology from the academic session 2020-2022.

23/8/22

Thesis advisor
Dr Sourav Sarkar
School of Materials Science and Nanotechnology
Jadavpur University,
Kolkata-700 032

Dr. Sourav Sarkar
Director
Associate Professor
School of Materials Science & Nanotechnology
Jadavpur University
Kolkata - 700032

23/8/22

Director
School of Materials Science and Nanotechnology
Jadavpur University
Kolkata-700 032

Dr. Sourav Sarkar
Director
Associate Professor
School of Materials Science & Nanotechnology
Jadavpur University
Kolkata - 700032

24/08/2022

Dean
Faculty Council of Interdisciplinary Studies, Law and Management
Jadavpur University,
Kolkata-700 032

Dean
Faculty of Interdisciplinary Studies
Law & Management
Jadavpur University, Kolkata-700032

M.Tech (Nano Science and Technology)
Course affiliated to:
Faculty of Interdisciplinary Studies,
Law and Management
Jadavpur University
Kolkata, India

CERTIFICATE OF APPROVAL

I hereby endorse the foregoing thesis as an engineering study, conducted and presented in a manner satisfactory enough to justify its acceptance as an engineering study, in order to obtain the degree for which it has been submitted. This approval does not endorse or approve any statement made, opinion expressed or conclusion drawn therein, but merely approves the thesis for the purpose for which it has been submitted.

Committee of the final examination
for evaluation of the Thesis

_____

_____

_____

_____

** Only in case the thesis is approved.

DECLARATION OF ORIGINALITY AND COMPLIANCE OF ACADEMIC ETHICS

I hereby declare that this thesis contains a literature survey and original research work by the undersigned candidate for the Master of Technology (Nano Science and Technology) program during the academic year 2020-2022.

The information in this document has been gathered and presented according to academic standards and ethical conduct.

I also declare that I have cited and referred to all materials and results that are not original to this work as required by these rules and conduct.

Name: **TANAY TOPPO**

Roll Number: **M4NST22016**

Registration Number: **136366 of 2016-17**

Thesis Title: Core and edge-specific functionalisation of graphene quantum dots to improve amino acid sensing.

SIGNATURE **DATE**

Dedicated to my parents

ACKNOWLEDGEMENT

I sincerely thank Dr Sourav Sarkar, my adviser, for his unwavering encouragement, passion, and vast expertise during my Master's studies and research. He helped me every step of the way as I wrote my thesis. My entire study project was driven by his insightful comments, and I am appreciative of that. Additionally, I'd like to thank Prof. (Dr). Kalyan Kumar Chattopadhyay and the Thin Film and Nano Science Lab as well as the Nanoscience and Nanotechnology Lab for creating a welcoming work atmosphere for me.

My appreciation is extended to my mentor, Mr Dipayan Roy, for his guidance, aid with all of my project-related challenges, and for collaborating with me to make it what it is today.

I sincerely appreciate the help, encouragement, recommendations, and counsel that Prof (Dr.) Kalyan Kumar Chattopadhyay, Dr Sourav Sarkar, Dr Mahua Ghosh, and Dr Chandan Kumar Ghosh provided. They created a supportive and productive learning environment, and their enthusiasm encouraged me to follow the study project with great passion.

My seniors, Sk Najes Riaz, Ankita Chandra, Dimitra Das, Antika Das, Karamjyoti Panigrahi, Nabanita Sen, Suvankar Mondal, Ratna Sarkar, Bikram Kumar Das, Souvik Bhattacharjee Anibrata Banerjee, Suvankar Poddar, Suvra Pal and Arnab Das deserve my deepest appreciation for making my project such a wonderful experience. I sincerely appreciate the help and support that Jaanvvi Kirpalani, Shahena Shah, Manoj Pal, Md Imran Ansari, Manas Thakur, Dipa Bala Sarkar, Swagata Das, and my other classmates and juniors gave me throughout this course. Without their help, I would not have been able to finish my project. My expressions of thanks to them are insufficient in light of their extraordinary assistance.

Finally, I want to sincerely thank my parents and all of my supporters for their love and support.

Table of Contents

Abstract

The study given in the thesis "Core and edge-specific functionalization of graphene quantum dots to improve amino acid sensing and metal sensing." is primarily concerned with two concerns: first, the synthesis of Graphene Quantum Dots, and second, the sensing of metals and amino acids.

Graphene quantum dots (GQDs) are zero-dimensional carbon allotropes that are made up of a monolayer or a few layers of graphene and have excellent characteristics. GQDs have both the properties of carbon dots (CDs) and graphene. GQDs can be mixed with other materials to create nanocomposites with outstanding characteristics and performance. Moreover, GQDs are environmentally beneficial due to their non-toxic and biologically inert qualities, which have piqued the interest of academic and industrial researchers worldwide. The primary goal is to synthesize Nitrogen-doped Graphene Quantum Dots and Graphene Quantum Dots using hydrothermal synthesis. Their structural and optical properties have been researched and characterized. Nitrogen has been doped into GQDs to broaden the material's functionalities. The control of its size and form was achieved by adjusting the time in the preparation parameter.

GQDs and NGQDs have been thoroughly discussed in all areas, including their prospective uses in metal and amino acid sensing. Thus, Graphene Quantum Dots are used in biotechnology and as sensing elements in this course of work.

Chapter 1

Introduction

1.1 Nanostructure

Nanostructured materials [1-4] are of interest because they can bridge the gap between the bulk and molecular levels, opening up new applications, particularly in electronics, optoelectronics, and biology. When a solid demonstrates a distinct variation of optical and electronic properties with a particle size variation of 100 nm, it is referred to as a nanostructure, and it is classified as 1. two-dimensional, e.g., thin films or quantum wells, 2. one-dimensional, e.g., quantum wires, or 3. zero-dimensional or dots.

1.2 Carbon Allotropes

Carbon is a remarkable material that is the most abundant material present in the form of coal, and it is one of the causes of the existence of life on Earth. It has lately astounded us once more in the form of graphene [5].

As shown in Fig. 1, graphitic forms of carbon include zero-dimension (0D), one-dimension (1D), two-dimension (2D), and three-dimension (3D) graphite.

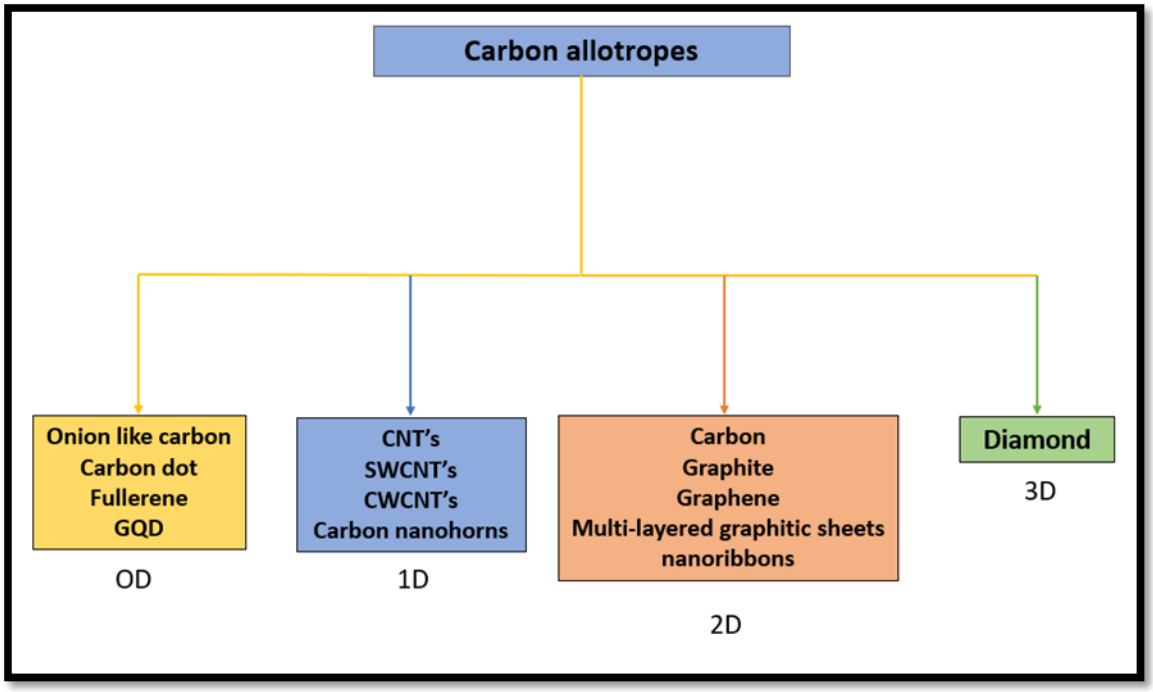

Fig 1. Classification of Carbon materials

1.2.1 Graphene

Because of the van der Waals force between the layers, 2D graphene is a single-layered nanomaterial ripped off from multi-layered graphite. The strongest and thinnest material ever measured in the Universe is one atom thick carbon material. Graphene was discovered in 2004 by a community of researchers from Manchester University in the United Kingdom, and it was hailed as the miracle substance of the twenty-first century [6-9]. Graphene and graphene-related materials encompass many nanostructures with identical nomenclature, indicating that the carbon material contains a single or a few monolayers of graphene. Currently, various improved technologies for careful handling and manufacture of graphene and its derivatives are available, yielding products with varying sizes and waste content such as C, O, and H or surface groups such as carboxyl, carbonyl, epoxy, and hydroxyl [10-12].

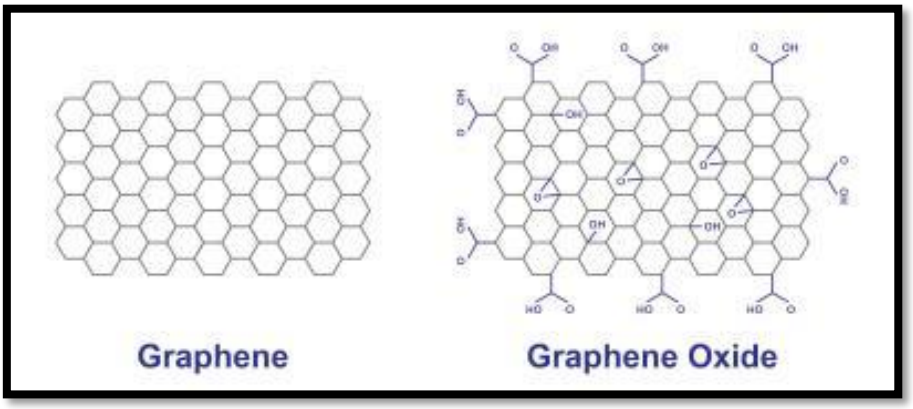

1.2.2 Graphene Oxide

Because graphene is both expensive and difficult to generate, tremendous efforts are being made to develop efficient yet low-cost methods of producing and utilizing graphene derivatives or related materials. Graphene oxide (GO) is one of these materials; it is a single-atomic layered substance produced by the intense oxidation of graphite, a cheap and abundant material. Graphene oxide is an oxidized version of graphene that has been impregnated with oxygen-containing groups. It is considered simple to treat because it dissolves in water (and other solvents), and it can even be used to produce graphene [13]. Although graphene oxide is a good conductor, procedures exist to dispute its qualities. It is generally offered as a powder, dispersed, or substrate coating.

1.3 Quantum Dots

Quantum dots (QD) are human-made nanometer-scale semiconductor crystals composed of elements from groups II to VI or III to V. They are described as particles with physical dimensions smaller than the exciton Bohr radius. When exposed to UV light, these semiconducting nanoparticles can emit a range of colours. These nanoparticles of synthetic semiconductors are employed in composites, solar cells, and fluorescent biological labeling [14,15]. Many fundamental features in the nanometer range are size dependent, therefore much attention has been paid to the optoelectronic properties of nanostructured semiconductors or quantum dots over the last two decades.

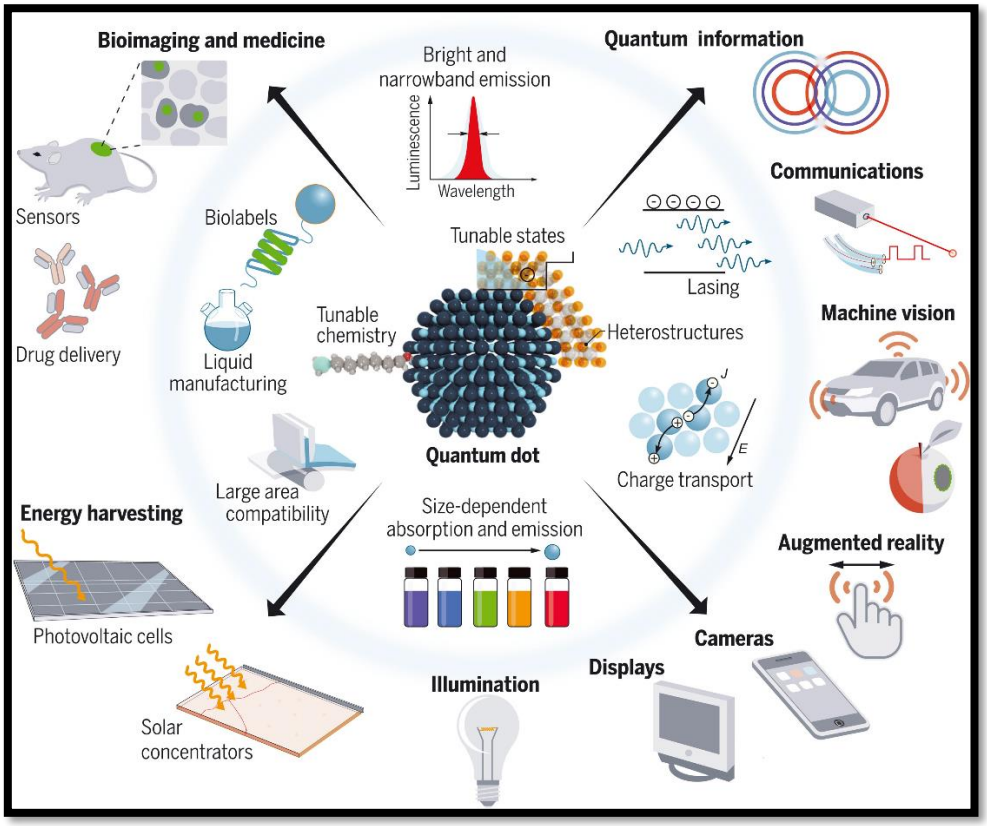

1.3.1 Carbon Dots and types

Carbon dots (CDs) are a catch-all term for a variety of carbon materials such as carbon quantum dots (CQDs), graphene quantum dots (GQDs), carbon nanodots (CNDs), and carbonized polymer dots (CPDs). These CDs family members are characterized according to their particular characteristics, surface groups, and carbon core structures [16,17].

1.3.2 Doping of Carbon Dots

The size of Carbon dots is typically controlled by the concentration of reactants, reaction temperature, duration, surfactants, additives, and so on. The hydrothermal approach, for example, was utilized to create extremely luminous Carbon dots from orange juice [18], glucose [19], banana juice [20], citric acid [21], and other liquids. Until now, the bulk of studies has reported the production of blue-emitting Carbon dots with excitation-dependent emission spectra. Furthermore, the emission spectra of Carbon dots can be modified by doping with elements such as nitrogen (N), sulphur (S), phosphorus (P), boron (B), or mixtures of these elements [22-26]. It has been demonstrated that doping Carbon dots increases fluorescence and shifts emission spectra. Fluorescent Carbon dots with green emission spectra, for example, have been reported and used for sensing and cell imaging [27]. Carbon dot's electronic structures can be altered by inserting atomic impurities, resulting in n-type or p-type carriers. As a result, by applying different types and amounts of doping atoms, their optical and electrical properties can be modified.

1.4 Graphene Quantum Dots

Over the last decade, researchers have attempted to successfully create 0D GQDs in 2D graphene lines. GQDs are made up of a monolayer or several monolayers of graphene (smaller than 100 nm in size) that arise related to quantum confinement and edge effects. GQDs are made from carbon-rich substrates like fullerene, glucose, graphite, graphene oxide (GO), carbon nanotubes (CNTs), and carbon fibres (CFs) [28].

1.4.1 Nitrogen-doped Graphene Quantum Dots

Nitrogen doping is a viable approach for modifying the chemical, electrical, and structural functions of graphene (G) and graphene quantum dots (GQDs) to improve their properties in energy and environmental applications. This research examines alternative methods for producing nitrogen-doped graphene (N-G) and nitrogen-doped graphene quantum dots (N-GQDs). ; N-G and N-GQDs have been synthesized using thermal, ultrasonic, solvothermal, hydrothermal, and electron-beam techniques. These nitrogen-doped carbon compounds are analyzed to determine their structural configurations to outperform graphene or graphene quantum dots in their applications [29].

1.4.2 Properties

i. Physical and chemical stability
ii. Possess a high surface-to-mass ratio.
iii. Because of the functional groups near the margins, it is easily distributed in the water.
iv. GQD fluorescence emission can span a wide spectral range, including UV, visible, and infrared. The origin of GQD fluorescence emission is a matter of discussion, as it has been linked to quantum confinement effects, defect states, and functional groups [30-31], which may be affected by the pH of water when GQDs are disseminated [32].
v. Their electronic orientation is highly sensitive to the crystallographic orientation of their edges; for instance, zigzag-edge GQDs with a diameter of 7-8 nm exhibit metallic properties. [33]
vi. Generally, as the number of graphene layers or carbon atoms per graphene layer increases, so does the energy gap. [34]

1.4.3 Application

i. **Sensors:** GQDs can act as good sensing materials due to their high electron mobility and fast reactivity, making them excellent candidates for sensing applications. GQDs have previously been investigated for applications such as field-effect transistors, photovoltaic, light-emitting diodes, electrochemical sensors, glucose sensors, PL sensors, ECL sensors, bioimaging, and bio-labelling [35-37].

ii. **Bio-medical:** GQDs are used in bio-imaging, bio-sensing, and drug delivery systems.

iii. **Energy:** Quantum dots have applications in energy storage as supercapacitors and lithium-ion batteries, as well as energy conversion as solar cells.

iv. **Catalytic:** GQDs have high catalytic activity and are widely used as a catalyst in processes such as photocatalytic hydrogen evolution and CO_2 reduction, electrocatalytic oxygen reduction, water splitting and CO_2 reduction, and photoelectron catalysis [38].

1.4.4 Drawbacks

i. CdSe-based quantum dots are extremely hazardous and necessitate a stable polymer shell.
ii. The shells can change the optical properties, and it is difficult to manage the particle size.
iii. The degradation of quantum dots within live organisms has been investigated.
iv. Overall conversion efficiency is decreased.
v. Operation at a lower temperature.
vi. Productivity of devices
vii. De-coherence [39].

1.4.5 Leftover work

More bio-imaging and logic gate applications are possible using quantum dots. Quantum dot nanoprobes can aid in bioimaging and organ perception. Quantum dots can play an important role in cancer research and help to establish a new route. To date, the majority of reported PL colours of GQDs ranged from blue to yellow [40]. GQDs' limited spectrum coverage limits their usage in optoelectronic devices. Extending GQD spectral coverage to all visible wavelengths and even near-infrared (NIR) is an important subject of future research. The NIR PL spectrum was achieved by several groups [41], [42], and [43] by doping nitrogen into GQDs. Once the aforementioned problems are overcome, the future of GQDs looks brighter.

Reference

1. Henglein, A. Small-particle research-physicochemical properties of extremely small colloidal metal and semiconductor particles. Chem. Rev. 1989, 89, 1861–1873.
2. Trindade, T.; O'Brien, P.; Pickett, N.L. Nanocrystalline semiconductors: Synthesis, properties, and perspectives. Chem. Mater. 2001, 13, 3843–3858.
3. Kuchibhatla, S.; Karakoti, A.S.; Bera, D.; Seal, S. One dimensional nanostructured materials. Prog. Mater. Sci. 2007, 52, 699–913.
4. Bera, D.; Kuiry, S.C.; Seal, S. Synthesis of nanostructured materials using template-assisted electrodeposition. JOM 2004, 56, 49–53.
5. P. Wick, A. E. Louw-Gaume, M. Kucki, H. F. Krug, K. Kostarelos, B. Fadeel, K. A. Dawson, A. Salvati, E. Vazquez, L. Ballerini, M. Tretiach, E. Flahaut, L. Gauthier, M. Prato and A. Bianco, Classification framework for graphene-based materials, Angew. Chem., Int. Ed., 2014,53(30), 7714–7718.
6. M. I. Katsnelson, Graphene: Carbon in two dimensions, Mater. Today, 2007, 10(1–2), 20–27.
7. S. Alwarappan and A. Kumar, Graphene-based materials: Science and Technology, Chapter 1: Graphene an introduction, Taylor & Francis group, CRC Press, London, New York 2014.
8. K. Deshmukh and G. M. Joshi, Embedded capacitor applications of graphene oxide reinforced poly(3,4-ethyl)-tetramethacrylate(PEDOT-TMA)composites, J.Mater.Sci.:Mater. Electron., 2015, 26, 5896–5909.
9. G. J. Thangamani, K. Deshmukh, K. K. Sadasivuni, K. Chidambaram, M. B. Ahamed, D. Ponnamma, M. A. A. AlMaadeed and S. K. K. Pasha, Recent advances in electrochemical biosensor and gas sensors based on graphene and carbon nanotubes (CNT) – a review, Adv. Mater. Lett., 2017, 8, 196–205.
10. K. K. Sadasivuni, D. Ponnamma, S. Thomas and Y. Grohens, Evolution from graphite to graphene elastomer composites, Prog. Polym. Sci., 2014, 39(4), 749–780.
11. K. Deshmukh, M. B. Ahamed, S. Sankaran, S. K. K. Pasha, K. K. Sadasivuni, D. Ponnamma and M. A. A. AlMaadeed, Studies on the mechanical, morphological and electrical properties of highly dispersible graphene oxide reinforced polypyrrole and polyvinyl alcohol blend composites, Mater. Today: Proc., 2018, 5, 8744–8752.

12. K. Deshmukh, S. Sankaran, M. B. Ahamed, S. K. K. Pasha, K. K. Sadasivuni, D. Ponnamma and M. A. A. AlMaadeed, Studies on the electrical properties of graphene oxide reinforced poly(4-styrene sulfonic acid) and polyvinyl alcohol blend composites, Int. J. Nanosci., 2018, 17, 1760005–1760013.
13. Gao, Wei.Springer, Cham, 2015. 61-95
14. Chan WC, Maxwell DJ, Gao X, Bailey RE, Han M: Luminescent quantum dots for multiplexed biological detection and imaging. Curr Opin Biotechnol 2002, 13(1):40–46.
15. https://www.nanowerk.com/what_are_quantum_dots.php#:~:text=Quantum%20dots%20(QDs)%20are%20man,cells%20and%20fluorescent%20biological%20labels.
16. Xia C., Zhu S., Feng T., Yang M., Yang B. Evolution and synthesis of carbon dots: From carbon dots to carbonized polymer dots. Adv. Sci. 2019;6:1901316. doi: 10.1002/advs.201901316.
17. Namdari P., Negahdari B., Eatemadi A. Synthesis, properties and biomedical applications of carbon-based quantum dots: An updated review. Biomed. Pharmacother. 2017;87:209–222. doi: 10.1016/j.biopha.2016.12.108.
18. Sahu S., Behera B., Maiti T.K., Mohapatra S. Simple one-step synthesis of highly luminescent carbon dots from orange juice: Application as excellent bio-imaging agents. Chem. Commun. 2012;48:8835–8837. doi: 10.1039/c2cc33796g.
19. Atabaev S. Size-tunable carbon nanoparticles with excitation-independent fluorescent properties. Mater. Today Proc. 2017;4:4896–4899. doi: 10.1016/j.matpr.2017.04.092.
20. De B., Karak N. A green and facile approach for the synthesis of water-soluble fluorescent carbon dots from banana juice. RSC Adv. 2013;3:8286–8290. doi: 10.1039/c3ra00088e.
21. Zhou M., Zhou Z., Gong A., Zhang Y., Li Q. Synthesis of highly photoluminescent carbon dots via citric acid and Tris for iron(III) ions sensors and bioimaging. Talanta. 2015;143:107–113.
22. Zhou J., Shan X., Ma J., Gu Y., Qian Z., Chen J., Feng H. Facile synthesis of P-doped carbon quantum dots with highly efficient photoluminescence. RSC Adv. 2014;4:5465–5468. doi: 10.1039/c3ra45294h.
23. Dong Y., Pang H., Yang H.B., Guo C., Shao J., Chi Y., Li C.M., Yu T. Carbon-based dots co-doped with nitrogen and sulfur for high quantum yield and excitation-independent emission. Angew. Chem. Int. Ed. 2013;52:7800–7804. doi: 10.1002/anie.201301114.

24. Bourlinos A.B., Trivizas G., Karakassides M.A., Baikousi M., Kouloumpis A., Gournis D., Bakandritsos A., Hola K., Kozak O., Zboril R., et al. Green and simple route toward boron doped carbon dots with significantly enhanced non-linear optical properties. Carbon. 2015;83:173–179. doi: 10.1016/j.carbon.2014.11.032.
25. Barman M.K., Jana B., Bhattacharyya S., Patra A. Photophysical Properties of Doped Carbon Dots (N, P, and B) and Their Influence on Electron/Hole Transfer in Carbon Dots—Nickel (II) Phthalocyanine Conjugates. J. Phys. Chem. C. 2014;118:20034–20041. doi: 10.1021/jp507080c.
26. Xu Q., Pu P., Zhao J., Dong C., Gao C., Chen Y., Chen J., Liu Y., Zhou H. Preparation of highly photoluminescent sulfur-doped carbon dots for Fe(III) detection. J. Mater. Chem. A. 2015;3:542–546. doi: 10.1039/C4TA05483K.
27. Zhang J., Zhao X., Xian M., Dong C., Shuang S. Folic acid-conjugated green luminescent carbon dots as a nanoprobe for identifying folate receptor-positive cancer cells. Talanta. 2018;183:39–47. doi: 10.1016/j.talanta.2018.02.009.
28. S. Tajik, Z. Dourandish, K. Zhang, H. Beitollahi, O. V. Le, H. W. Jang and M. Shokouhimehr, Carbon and graphene quantum dots: a review on syntheses, characterization, biological and sensing applications for neurotransmitter determination, RSC Adv., 2020, 10, 15406–15429.
29. Nitrogen-doped graphene and graphene quantum dots: A review on synthesis and applications in energy, sensors and environment
Manpreet Kaur, Manmeet Kaur, Virender K.Sharma
30. Pan, Dengyu; Zhang, Jingchun; Li, Zhen; Wu, Minghong (2010). "Hydrothermal Route for Cutting Graphene Sheets into Blue-Luminescent Graphene Quantum Dots". Advanced Materials. 22 (6): 734–738. doi:10.1002/adma.200902825
31. Wang, Shujun; Cole, Ivan S.; Zhao, Dongyuan; Li, Qin (2016). "The dual roles of functional groups in the photoluminescence of graphene quantum dots". Nanoscale. 8 (14): 7449–7458. Bibcode:2016Nanos...8.7449W. doi:10.1039/C5NR07042B. hdl:10072/142465. PMID 26731007.
32. Wu, Zhu Lian; Gao, Ming Xuan; Wang, Ting Ting; Wan, Xiao Yan; Zheng, Lin Ling; Huang, Cheng Zhi (2014). "A general quantitative pH sensor developed with dicyandiamide N-doped high quantum yield graphene quantum dots". Nanoscale. 6 (7): 3868–3874. Bibcode:2014Nanos...6.3868W. doi:10.1039/C3NR06353D. PMID 24589665.

33. Ritter, Kyle A; Lyding, Joseph W (2009). "The influence of edge structure on the electronic properties of graphene quantum dots and nanoribbons". Nature Materials. 8 (3): 235–42. Bibcode:2009NatMa...8..235R. doi:10.1038/nmat2378. PMID 19219032
34. Wimmenauer, Christian; Scheller, Julienne; Fasbender, Stefan; Heinzel, Thomas (2019). "Single-particle energy – and optical absorption – spectra of multilayer graphene quantum dots". Superlattices and Microstructures. 132: 106171. doi:10.1016/j.spmi.2019.106171.
35. M. K. Kumawat, M. Thakur, R. B. Gurung and R. Srivastava, Graphene quantum dots from mangifera indica: Application in near-infrared bioimaging and intracellular nano-thermometry, ACS Sustainable Chem. Eng., 2017, 5(2), 1382–1392.
36. X. Liu, W. Na, Z. Liu, X. Chen and X. Su, Fluorescence turn-on probe based on polypyrrole/graphene quantum composites for selective and sensitive detection of paracetamol and ascorbic acid, Biosens. Bioelectron., 2017, 98, 222–226.
37. Y. H. Li, L. Zhang, J. Huang, R. L. Liang and J. D. Qiu, Fluorescent graphene quantum dots with a boronic acid appended bipyridinium salt to sense monosaccharides in aqueous solution, Chem. Commun., 2013, 49(45), 5180–5182.
38. T.-F. Yeh, C.-Y. Teng, S.-J. Chen and H. Teng, Nitrogen-doped Graphene Oxide Quantum Dots as Photocatalysts for Overall Water-Splitting Under Visible Light Illumination, Adv. Mater., 2014, 26, 3297–3303.
39. https://www.rfwireless-world.com/Terminology/Advantages-and-Disadvantages-of-Quantum-Dots.html
40. L. Li, G. Wu, G. Yang, J. Peng, J. Zhao, J.-J. Zhu Focusing on luminescent graphene quantum dots: current status and future perspectives Nanoscale, 5 (2013), pp. 4015-4039
41. L. Tang, R. Ji, X. Li, G. Bai, C.P. Liu, J. Hao, J. Lin, H. Jiang, K.S. Teng, Z. Yang, S.P. Lau Deep ultraviolet to near-infrared emission and photoresponse in layered N-doped graphene quantum dots ACS Nano, 6 (2014), pp. 6312-6320
42. T. Gao, X. Wang, L.-Y. Yang, H. He, X.-X. Ba, J. Zhao, F.-L. Jiang, Y. Liu Red, yellow, and blue luminescence by graphene quantum dots: syntheses, mechanism, and cellular imaging ACS Appl. Mater. Interfaces, 29 (2017), pp. 24846-24856
43. Y. Dong, J. Shao, C. Chen, H. Li, R. Wang, Y. Chi, X. Lin, G. Chen Blue luminescent graphene quantum dots and graphene oxide prepared by tuning the carbonization degree of citric acid Carbon, 12 (2012), pp. 4738-4743

CHAPTER 2

NANOTECHNOLOGY

&

NANOMATERIALS

2.1 Introduction

The prefix 'nano' refers to a Greek prefix that means 'dwarf' or very small and represents one thousand millionths of a metre (10^{-9} m). We must differentiate between nanoscience and nanotechnology. Nanoscience is the study of structures and chemicals on nanometer scales ranging from 1 to 100 nm, and nanotechnology is the technology that uses in practical applications such as devices [1]. In comparison, a single human hair is 60,000 nm thick and the DNA double helix has a radius of 1 nm (Figure 1) [2].

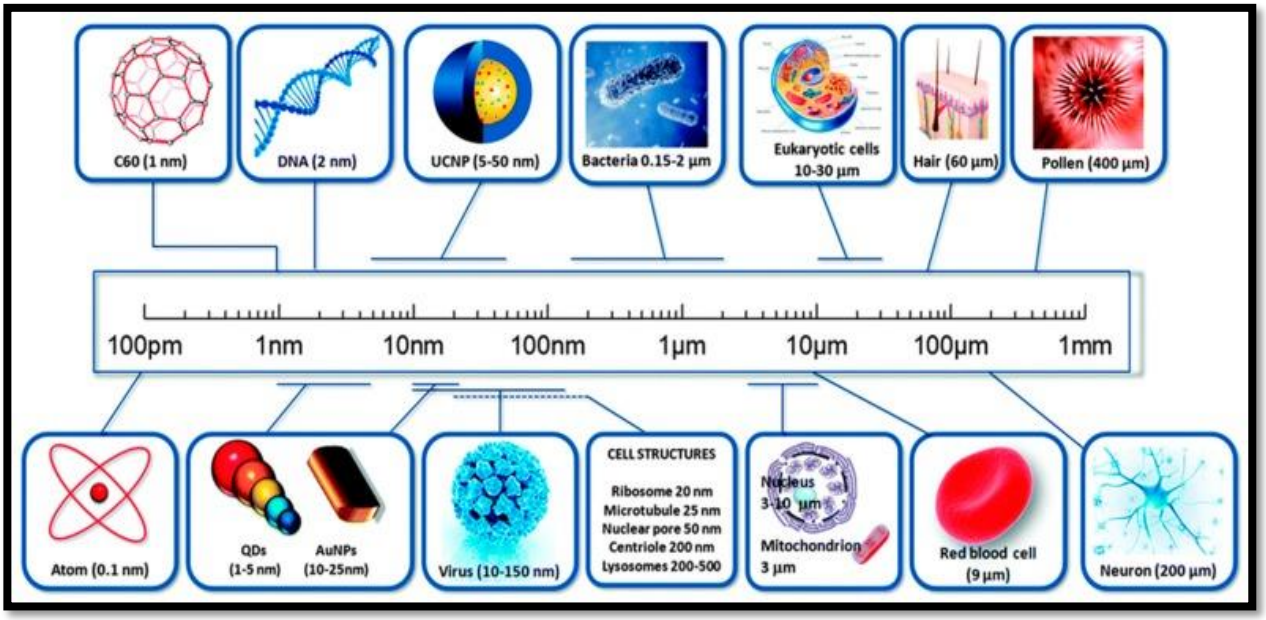

Figure 1: A comparison of sizes of nanomaterial. Reproduced with permission from reference [2].

Nanotechnology is one of the most promising 21st-century technologies. It is the ability to apply nanoscience theory by viewing, measuring, manipulating, assembling, regulating, and creating materials on a nanoscale scale. Nanotechnology is defined by the National Nanotechnology Initiative (NNI) in the United States as "a science, engineering, and technology conducted at the nanoscale (1 to 100 nm), where unique phenomena enable novel applications in a wide range of fields, from chemistry, physics, and biology, to medicine, engineering, and electronics."

Nanoscience is the application of physics, materials science, and biology to the manipulation of materials at the atomic and molecular levels, whereas nanotechnology is the ability to observe, detect, modify, construct, regulate, and manufacture matter at the nanometer scale [3].

2.2 Properties of Nanomaterial

1. Dimension: at least one dimension ranging from 1 to 100 nanometres (nm).

2. Methodology: developed with approaches that demonstrate fundamental control over the physical and chemical properties of molecular-scale formations.

3. Building block property: They can be merged to construct larger structures. In general, nanoscience is relatively natural in microbiological sciences because the sizes of many bioparticles dealt with (such as enzymes, viruses, and so on) fall within the nanometer range.

4. Large area/volume ratio: The surface area/volume ratio has a greater impact on certain properties of nanoparticles than on bulk particles.

5. Interfacial layer: The interfacial layer created by ions and molecules from the medium that are within a few atomic diameters of the surface of each particle for nanoparticles dispersed in a medium of diverse compositions can conceal or change its chemical and physical properties. That layer is, in fact, an essential component of each nanoparticle.

2.3 Applications of Nanotechnology

Nanotechnology is being applied in a wide range of scientific domains, with a wide range of unique applications. When a particle is shrunk to the nanoscale, the properties of the substance change proportionally to its size. As a result, it creates new opportunities in a range of industries. There is greater surface area to react when the surface-to-volume ratio grows with size. The diameter or size of particles influences a variety of optical and mechanical qualities.

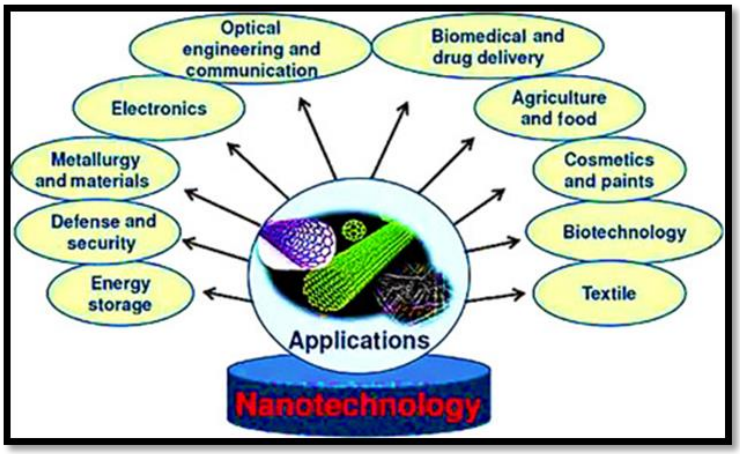

i. **Electronics:** In electronics, nanotechnology allows for faster, smaller, and more portable systems. Nanoelectronics improves electrical device capabilities, boosts memory chip density, and reduces power consumption and transistor size in integrated circuits.

ii. **Energy storage:** Nanotechnologies, such as novel ceramic, heat-resistant, and still flexible separators and high-performance electrode materials, can significantly improve the capacity and safety of lithium-ion batteries [4].

iii. **Biomedical and drug delivery:** Nanotechnology applications in several biology-related domains, such as diagnosis, medicinal delivery, and molecular imaging, are being extensively explored and yield promising results. In the realm of nano-oncology, remarkable progress has been made in enhancing the efficacy of standard chemotherapeutic medications for a variety of aggressive human tumours [5,6].

iv. **Defence and security:** Nanomaterials have the potential to make firearms lighter and with more ammunition. When these new technologies are combined, they may lead to guns that can automatically target and fire self-guided rounds if an attacker is identified. Nanorobots are capable of attacking and destroying weaponry, metals, and other objects [7].

Reference

1. Mansoori G., Fauzi Soelaiman T. Nanotechnology—An Introduction for the Standards Community. J. ASTM Int. 2005;2:1–22.

2. Gnach A., Lipinski T., Bednarkiewicz A., Rybka J., Capobianco J.A. Upconverting nanoparticles: Assessing the toxicity. Chem. Soc. Rev. 2015;44:1561–1584. doi: 10.1039/C4CS00177J.

3. The History of Nanoscience and Nanotechnology: From Chemical–Physical Applications to Nanomedicine. Samer Bayda,1,* Muhammad Adeel,2,3 Tiziano Tuccinardi,4 Marco Cordani,5 and Flavio Rizzolio2,6,*

4. Application of Nanotechnologies in the Energy Sector Volume 9 of the Technologielinie Hessen-Nanotech Publication Series of the Ministry of Economics, Energy, Transport and Regional Development – State of Hessen

5. Lee P.Y., Wong K.K.Y. Nanomedicine: A new frontier in cancer therapeutics. Curr. Drug Deliv. 2011;8:245–253.

6. Yuan Y., Gu Z., Yao C., Luo D., Yang D. Nucleic Acid–Based Functional Nanomaterials as Advanced Cancer Therapeutics. Small. 2019;15:1900172.

7. Nanotechnology for Defense and Security Christian Ngo & Marcel H. Van de Voorde.

Chapter 3

Review of Past Work

&

Objective

3.1 Review of Graphene Quantum dot: General Idea

Ponomarenko and Geim [1] created graphene quantum dots (GQDs) in 2008, building on previous work on carbon dots (CDs) by Xu [2] et al. in 2004. GQDs vary from CDs in that they have graphene lattices within the dots that are smaller than 100 nm in size and fewer than 10 layers thick [3]. CDs are typically quasi-spherical carbon nanoparticles with diameters smaller than 10 nm [3]. Because of the quantum confinement effect, GQDs have numerous novel properties, such as their distinctive fluorescence properties found by Pan [4] et al. in 2010. If GQDs are to be used in a variety of applications, the ability to adjust their properties is critical. Modification of GQD characteristics through doping was initially examined in 2012 by Zhao [5] and collaborators, who used nitrogen as a dopant in GQDs. Furthermore, GQDs are more soluble than CNTs. This is owing to the significant edge effect of GQDs, which may be adjusted by functional groups, as opposed to CNTs, which are confined by their one-dimensional nature. Previous theoretical calculations, as well as optical and electrical investigations, have shown that bandgaps exist in GQDs. Semi-metal graphene can be converted into semiconductor or insulator GQDs. Because of the expansion of the bandgap in GQDs, the broadening of graphene's optical absorption has resulted in a greater energy spectrum. Due to the distinctive edge and quantum confinement effects, GQDs have different chemical and physical properties when compared to other carbon-based materials such as CD, CNTs, fullerene, and graphene, among others [6]. GQDs have numerous significant properties, including stable PL, non-toxicity, excellent solubility, surface grafting, biocompatibility, and inertness [7].

3.1.1 Different methods to synthesize GQD's

According to the precursor material, GQDs preparation methods developed in recent years can be categorized into two categories: top-down and bottom-up. The top-down method refers to the direct cutting of graphene-related materials such as graphene [8], graphene oxide [9], carbon nanotubes [10], carbon fibres [11], carbon black [12], graphite powder [13], and coal [14] into quantum size by various methods, as indicated in the centre of Fig. 2. Bottom-up approaches use sequential chemical reactions to convert graphene-like smaller polycyclic

aromatic hydrocarbons (PAHs) molecular precursors such as benzene [15], hexa-peri-hexabenzocoronene [16], glucose [17], and fullerene [18] to GQDs.

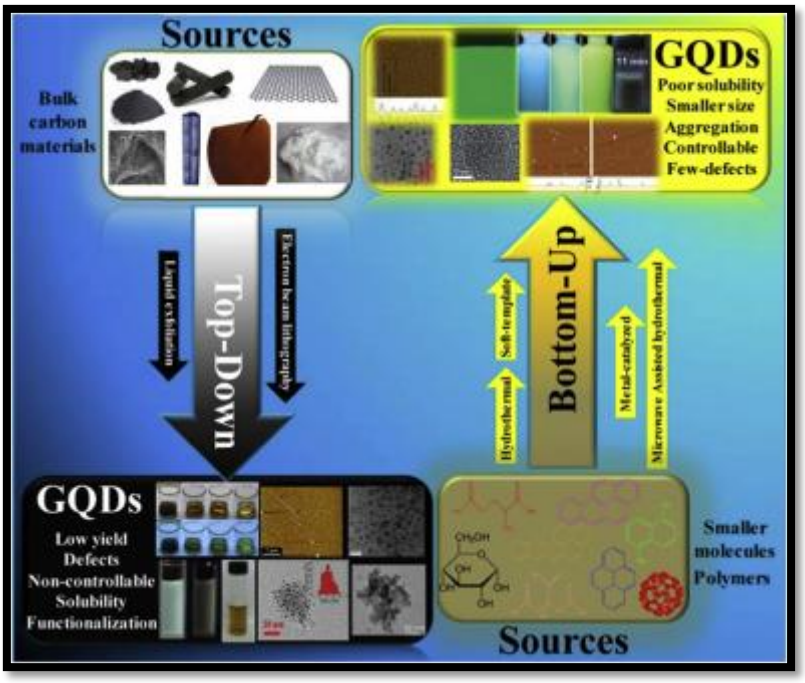

Fig. Techniques to synthesize GQD.

a. **Bottom-Up:** Bottom-up approaches, as previously stated, are based on the transformation of sources such as graphene-like smaller polycyclic aromatic hydrocarbons (PAHs) and suitable molecules into GQDs. However, depending on how external energy is delivered and fabrication properties, this approach can be split into four major routes: hydrothermal method, microwave-assisted hydrothermal method, soft-template method, and metal-catalyzed method [6].
b. **Top-Down:** According to the link between precursors and products, the top-down approach is the inverse of the bottom-up method. The top-down technique typically fabricates GQDs by physically or chemically breaking down the bulk material. The first GQDs were created using this method, demonstrating that top-down approaches are particularly useful in the identification of novel materials and the study of their structure and properties. Among top-down routes, liquid exfoliation methods (hydrothermal, electrochemical, oxidation, and ultrasonic, for example) and electron beam lithography methods are widely utilized. Other, less popular approaches, such as magnetron sputtering, will also be discussed in this section [6].

Source	Diameter (nm)	PLQY	Colour of PL	Product yield	Advantages	Disadvantages	Ref
CA (Citric Acid)	~15	9.0%	blue	__	high yield, easy to dope	small size, long period	[19]
CA+EDA (EDA- ethylenediamine)	5-10	75.2%	blue	60% - 70%	__	__	[20]
CA	2-8	34%	blue	__	__	__	[21]
Pyrene	3.5 ± 0.6	23%	green	63%	__	__	[22]
1,5-dinitronaphthalene	1.5	__	Green-yellow	__	__	__	[23]
l-glutamic acid	4.66 ± 1.24	54.5%	NIR	__	__	__	[24]
CA+Tris-HMA(tris(hydroxymethyl) aminomethane)	0.5–4	59.2%	blue	__	__	__	[25]

Table: Properties of GQD's synthesized hydrothermally.

To meet industry demands, it is required to mass produce GQDs at a low cost. However, the product yield of GQDs using current preparation methods [26] is very low (usually 10%), thus innovative ways that can improve the product yield, such as the photo-Fenton reaction method (maximum yield of 45% [26]) and simple synthesis methodology employing coals [14], must be explored. The reported quantum yields (QYs) of GQDs are generally between 2% and 22.9% [26], which is significantly lower than the QYs of standard semiconductors.

3.1.2 Applications of GQD's

The properties of GQDs are vastly superior to those of traditional semiconductor quantum dots, implying a wide range of potential applications in solar cells, photodetectors, bioimaging, fluorescent agents, light-emitting diodes (LEDs), batteries, sensors, drug carriers, and photo-/electro-catalytic systems, among others. GQD research is still in its early stages, and many GQD difficulties have still to be addressed. Although GQDs have many major advantages and possible uses, more research to improve the material's characteristics is needed to meet the application criteria [6].

3.2 Objective

The primary goal of this thesis is to synthesize Graphene Quantum Dot and Nitrogen-doped Graphene Quantum Dots by a hydrothermal procedure and investigate their structural, optical, and morphological features. The manufactured GQDs will be used for amino acid and metal sensing, and we will also see excitation-dependent PL nature.

The following are our thesis objectives:

1. To synthesize Nitrogen-doped Graphene Quantum Dots using hydrothermal synthesis. It is also critical to determine the ideal synthesis conditions through optimization of synthesis parameters to build a successful technology approach for the pure phase of NGQD.

2. The hydrothermal control synthesis technique was used to create Graphene Quantum Dots. Determining the best synthesis circumstances through optimization of synthesis parameters is also critical for building a successful technology route for the pure phase of GQD.

3. This thesis also aims to characterize the as-synthesized GQD and NGQD using a UV-Vis Spectrophotometer, Photoluminescence, XPS, HRTEM and so on.

4. Finally, discovering applications for synthesised GQDs and NGQDs is a crucial priority.

Reference

1. L.A. Ponomarenko, F. Schedin, M.I. Katsnelson, R. Yang, E.W. Hill, K.S. Novoselov, A.K. Geim Chaotic dirac billiard in graphene quantum dots Science, 320 (2008), pp. 356-358
2. X.Y. Xu, R. Ray, Y.L. Gu, H.J. Ploehn, L. Gearheart, K. Raker, W.A. Scrivens Electrophoretic analysis and purification of fluorescent single-walled carbon nanotube fragments J. Am. Chem. Soc., 126 (2004), pp. 12736-12737
3. D. Wang, J.-F. Chen, L. Dai, Recent Advances in graphene quantum dots for fluorescence bioimaging from cells through tissues to animals Part. Part. Syst. Char, 5 (2015), pp. 515-523
4. D. Pan, J. Zhang, Z. Li, M. Wu Hydrothermal route for cutting graphene sheets into blue-Luminescent graphene quantum dots Adv. Mater., 6 (2010), pp. 734-738
5. Y. Zhao, C.G. Hu, Y. Hu, H.H. Cheng, G.Q. Shi, L.T. Qu A versatile, ultralight, nitrogen-doped graphene framework Angew. Chem. Int. Ed., 51 (2012), pp. 11371-11375
6. Graphene quantum dots from chemistry to applications P.Tian, L.Tang, K.S.Teng, S.P.Lau
7. S.Y. Lim, W. Shen, Z. Gao Carbon quantum dots and their applications Chem. Soc. Rev., 44 (2015), pp. 362-381
8. D. Pan, J. Zhang, Z. Li, M. Wu Hydrothermal route for cutting graphene sheets into blue-Luminescent graphene quantum dots Adv. Mater., 6 (2010), pp. 734-738
9. S. Kim, S.W. Hwang, M.-K. Kim, D.Y. Shin, D.H. Shin, C.O. Kim, S.B. Yang, J.H. Park, E. Hwang, S.-H. Choi, G. Ko, S. Sim, C. Sone, H.J. Choi, S. Bae, B.H. Hong Anomalous behaviours of visible luminescence from graphene quantum dots: interplay between size and shape ACS Nano, 9 (2012), pp. 8203-8208
10. Y. Dong, H. Pang, S. Ren, C. Chen, Y. Chi, T. Yu Etching single-wall carbon nanotubes into green and yellow single-layer graphene quantum dots Carbon, 64 (2013), pp. 245-251
11. J. Peng, W. Gao, B.K. Gupta, Z. Liu, R. Romero-Aburto, L. Ge, L. Song, L.B. Alemany, X. Zhan, G. Gao, S.A. Vithayathil, B.A. Kaipparettu, A.A. Marti, T. Hayashi, J.-J. Zhu, P.M. Ajayan Graphene quantum dots derived from carbon fibers Nano Lett., 2 (2012), pp. 844-849

12. Y. Dong, C. Chen, X. Zheng, L. Gao, Z. Cui, H. Yang, C. Guo, Y. Chi, C.M. Li One-step and high yield simultaneous preparation of single- and multi-layer graphene quantum dots from CX-72 carbon black J. Mater. Chem., 18 (2012), p. 8764
13. Y. Sun, S. Wang, C. Li, P. Luo, L. Tao, Y. Wei, G. Shi Large scale preparation of graphene quantum dots from graphite with tunable fluorescence properties Phys. Chem. Chem. Phys., 24 (2013), p. 9907
14. R.Q. Ye, C.S. Xiang, J. Lin, Z.W. Peng, K.W. Huang, Z. Yan, N.P. Cook, E.L.G. Samuel, C.C. Hwang, G.D. Ruan, G. Ceriotti, A.R.O. Raji, A.A. Marti, J.M. Tour Coal as an abundant source of graphene quantum dots Nat. Commun., 4 (2013), p. 2943
15. K. Habiba, V.I. Makarov, J. Avalos, M.J.F. Guinel, B.R. Weiner, G. Morell Luminescent graphene quantum dots fabricated by pulsed laser synthesis Carbon, 64 (2013), pp. 341-350
16. R. Liu, D. Wu, X. Feng, K. Müllen Bottom-up fabrication of photoluminescent graphene quantum dots with uniform morphology J. Am. Chem. Soc., 39 (2011), pp. 15221-15223
17. L. Tang, R. Ji, X. Li, G. Bai, C.P. Liu, J. Hao, J. Lin, H. Jiang, K.S. Teng, Z. Yang, S.P. Lau Deep ultraviolet to near-infrared emission and photoresponse in layered N-doped graphene quantum dots ACS Nano, 6 (2014), pp. 6312-6320
18. J. Lu, P.S.E. Yeo, C.K. Gan, P. Wu, K.P. Loh Transforming C-60 molecules into graphene quantum dots Nat. Nanotechnol., 4 (2011), pp. 247-252
19. Y. Dong, J. Shao, C. Chen, H. Li, R. Wang, Y. Chi, X. Lin, G. Chen Blue luminescent graphene quantum dots and graphene oxide prepared by tuning the carbonization degree of citric acid Carbon, 12 (2012), pp. 4738-4743
20. J. Gu, X. Zhang, A. Pang, J. Yang Facile synthesis and photoluminescence characteristics of blue-emitting nitrogen-doped graphene quantum dots Nanotechnology, 27 (16) (2016), p. 165704
21. A.B. Ganganboina, A.D. Chowdhury, R.-A. Doong N-Doped graphene quantum dots-decorated V2O5 nanosheet for fluorescence turn off–on detection of cysteine ACS Appl. Mater. Interfaces, 1 (2017), pp. 614-624
22. L. Wang, Y. Wang, T. Xu, H. Liao, C. Yao, Y. Liu, Z. Li, Z. Chen, D. Pan, L. Sun, M. Wu Gram-scale synthesis of single-crystalline graphene quantum dots with superior optical properties Nat. Commun., 5 (2014), p. 5357
23. X. Wu, F. Tian, W. Wang, J. Chen, M. Wu, J.X. Zhao Fabrication of highly fluorescent graphene quantum dots using L-glutamic acid for in vitro/in vivo imaging and sensing

J. Mater. Chem. C, 31 (2013), pp. 4676-46

24. X. Wu, F. Tian, W. Wang, J. Chen, M. Wu, J.X. Zhao Fabrication of highly fluorescent graphene quantum dots using L-glutamic acid for in vitro/in vivo imaging and sensing J. Mater. Chem. C, 31 (2013), pp. 4676-4684
25. L. Lin, M. Rong, S. Lu, X. Song, Y. Zhong, J. Yan, Y. Wang, X. Chen Facile synthesis of highly luminescent nitrogen-doped graphene quantum dots for the detection of 2,4,6-trinitrophenol in aqueous solution Nanoscale, 7 (2015), pp. 1872-1878
26. L. Li, G. Wu, G. Yang, J. Peng, J. Zhao, J.-J. Zhu Focusing on luminescent graphene quantum dots: current status and future perspectives Nanoscale, 5 (2013), pp. 4015-4039

Chapter 4

Amino acid sensing

&

Metal sensing

4.1 Amino acid sensing

The tremendous increase in electrochemistry research over the last decade has resulted in significant progress in utilising electrochemical techniques for analysing biological molecules. Amino acids are of particular importance due to their critical function in human health. Indeed, an imbalanced amino acid level is at the root of many metabolic and genetic illnesses, necessitating the development of accurate and dependable assessment tools [1]. This work uses amino acid sensing to determine the amount of amino acids in our body and then works accordingly. Because of the nutritional, biotechnological, and therapeutic importance of amino acids, a significant portion of the research is focused on developing practical and reliable analytical techniques for evaluating amino acids.

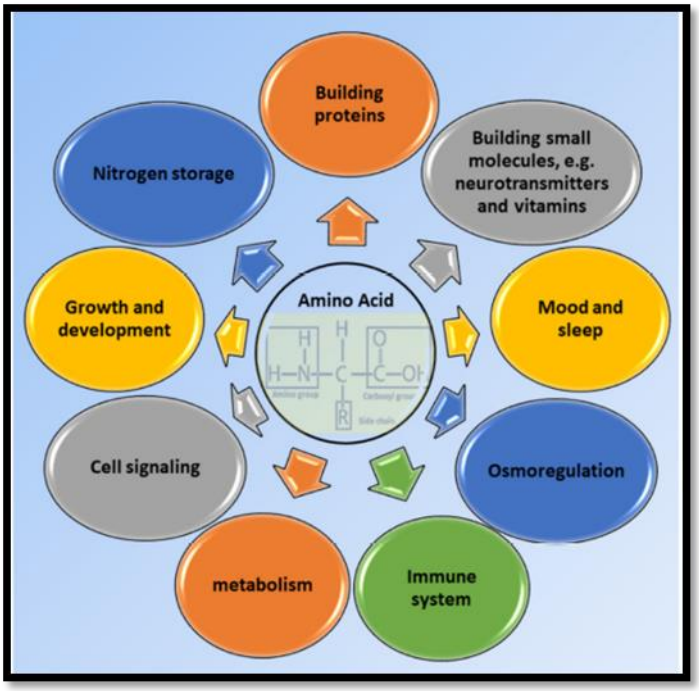

Small molecules and macromolecules are widely recognised as the fundamental building blocks of known life. Carbohydrates, proteins, nucleic acids, and lipids are the four major macromolecule classes, whereas amino acids, hormones, vitamins, neurotransmitters and metabolites, as well as various medications, are examples of tiny molecules. Thousands of proteins in our bodies are made up of 20 different amino acids, each of which has an amino group and a carboxyl group at each terminal [1]. Essential amino acids are nine amino acids that cannot be produced endogenously in the human body: methionine, tryptophan, histidine, phenylalanine, valine, threonine, lysine, leucine, and isoleucine. The rest, known as non-

essential amino acids, can be synthesised by our bodies either from glucose, e.g., glycine, glutamate, glutamine, alanine, aspartate, arginine, asparagine, proline, and serine, or from the metabolism of other amino acids, e.g., tyrosine from phenylalanine and cysteine from methionine [2]. These amino acids serve as building blocks and are required for the synthesis of a wide range of low-molecular-weight compounds, including glutathione, thyroid hormones, creatine, melatonin, serotonin, melanin and heme, which are known for their involvement in body function [3].

Amino acid	Body Function Importance	Industrial Importance
Arginine 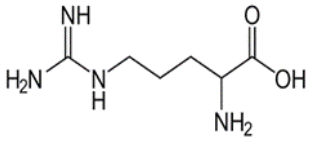	i. It is essential for an organism's metabolism. ii. It serves as a precursor for the creation of proteins. iii. It is an important amino acid for a young organism's proper growth and development. iv. Arginine is a conditionally necessary amino acid for adults, particularly in conditions such as trauma, burn injury, small-bowel resection, and renal failure. v. L-arginine supplementation benefits cardiovascular, pulmonary, immunological, and digestive functioning while also protecting against cancer in its early stages [2].	i. It has been shown to increase the production of growth hormones, prolactin, insulin, and glucagon. ii. It promotes muscle mass. iii. It promotes wound healing. iv. It is utilized as a nitric oxide precursor [3].
Cystine 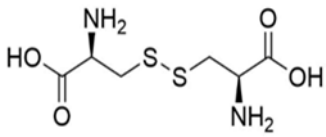	i. Because amino acids are amphoteric, they can serve as a biological buffer.	i. In the food business, cysteine is used as an antioxidant to preserve fruit juice and as an ingredient to

Cystine is composed of two cysteines.	ii. The cysteine Sulphydryl side chain is a powerful metal binder and is widely utilised in metal proteins to hold their metals in place. iii. Cysteine residues, due to their ability to create a disulphide bridge, help to stabilise the three-dimensional structure of proteins. iv. Cysteine is needed by the body to create glutathione, a powerful antioxidant. v. When needed, the body converts cysteine to glucose and uses it as an energy source. vi. Cysteine is essential for immune cell communication [4]. vii. Cysteine can be found in abundance in structural proteins such as keratin and collagen. viii. The WHO estimated cysteine consumption to be 4 mg/kg body weight per day needed for a healthy adult [5].	flour to improve dough kneading and as a baking processing help. ii. Cysteine can be found in products that help with skin lipid production and acne, as well as anti-dandruff shampoos. iii. Because of its high reactivity at neutral pH and low quantity in intracellular proteins, it is employed in selective protein purification [6]. iv. Cysteine is often utilised in the pharmaceutical industry as an antidote to mitigate the toxicity of other components, such as acetaminophen. v. Cysteine is replacing thioglycolic acid in the cosmetics sector due to its capacity to break the disulphide link in keratin in haircare products. vi. It is extensively utilised in the manufacture of nail-care products because it promotes fingernail growth and toughness [7].
Glycine	i. Glycine is a component of protein synthesis in the body.	i. Glycine is present in pet and animal food of USP quality.

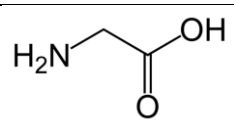	ii. Glycine is also involved in chemical signal transmission in the brain [8].	ii. Glycine is marketed to humans as a sweetener/taste enhancer. iii. Glycine is found in food supplements and protein beverages. iv. Some medication formulations contain glycine to increase drug absorption in the stomach. v. Glycine is used to buffer antacids, analgesics, antiperspirants, cosmetics, and toiletries. vi. Glycine is used to make rubber sponge goods, fertilizers, as well as metallic complexants [9].
Glutathione 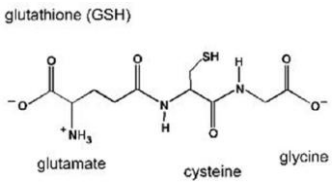 Glutathione is a chemical found in human cells that is composed of three amino acids: cysteine, glutamate, and glycine.	i. Glutathione is a powerful antioxidant in your body. ii. Glutathione is involved in a variety of chemical events in your body. iii. It also aids in the detoxification of substances, including those produced naturally by your body, as well as toxins and medicines [10].	i. Glutathione is the most commonly used as an oral medication to whiten the skin. It can also be applied as a cream [11]. ii. Glutathione, a naturally occurring grape antioxidant, helps protect the fragrance and flavour of white and rosé wines while also preventing premature aging [12].

4.1.1 Amino acid sensing using nanomaterials

A device based on single-walled carbon nanotubes (SWCNTs) to detect the important amino acids Glutamine and Tryptophan by evaluating changes in the device's various properties [13]. Utilizing fluorescent carbon quantum dots (CDs) produced hydrothermally, a fluorescent nanochemosensor has been developed to detect amino acids. Glycine (GLY), alanine (ALA), proline (PRO), aspartic acid (ASP), lysine (LYS), and histidine (HYS) are the amino acids it detects [14]. Carbon dots and nitrogen-doped carbon dots are employed to detect D-Pro and D-Ala calorimetrically. This nanoenzyme-based colorimetric technique makes detecting stomach cancer easier and faster [15].

4.2 Metal Sensing

Metal ions are required for life, but excessive concentrations pose harm to the intracellular environment. Metal ions play an important role in biology's structural and functional operations. Metal ion distribution and concentration variation in life are important subjects in bioanalytical chemistry, having implications for cell signalling, medicine development, and enzyme catalysis [16,17]. Anthropogenic activities have generated massive amounts of metal species through mining, industrial water discharge, corrosion, coal burning, and trash disposal, generating major environmental and health hazards [18]. As a result, metal identification is an important analytical task in biological and environmental research. Currently, metal analysis methods rely on devices like atomic absorption/emission and mass spectroscopy [19]. These procedures are costly, very accurate, and sensitive to industrial standards, but they need complicated sample processing, preventing them from being employed on-site, in real-time, or in situ. Metal sensors have been developed to supplement instrumentation analysis. Antibodies are a well-known sensing platform. Metal ions, on the other hand, are too tiny for direct antibody recognition and must be chelated first [20], which may affect selectivity. Furthermore, antibodies work best under physiological settings, whereas environmental samples may need to be identified under different conditions. Metal Sensors based on proteins and peptides were also demonstrated [21,22], but they are vulnerable to irreversible denaturation. Chemical metal

sensors rely heavily on fluorescent chelators that have been logically engineered. Metal ions are distinguished by their size, charge, and, in some cases, thiophilicity. A number of these probes for key metals like Ca^{2+} and Zn^{2+} have been marketed [23-29]. For decades, researchers have been investigating nucleotides and nucleic acids as metal ligands, primarily in the context of bioinorganic chemistry [30-33] and medicinal chemistry [34-35]. In the 1990s, efforts were made to control the evolution of metal-binding nucleic acids [36-37]. Since 1980, a key topic in ribozyme catalysis has been investigated [38-41].

cation	serum (mM)	intracellular matrix (mM)	urine (mM)	ref.
Na^{+}	142	12	95 ± 44	[42-43]
K^{+}	4.3	139	29 ± 17	[42-43]
Ca^{2+}	2.5	$<10^{-3}$(free)	15−20/24 h	[42,44]
Mg^{3+}	1.1(free)	1.6(free)	0.83 ± 0.09/24 h	[42,45]
Zn^{2+}	0.011	≤10−5 (free)	$6.7 \times 10^{-3} \pm 5.0 \times 10^{-4}$	[46-48]
Cu^{2+}	0.015	0.01−0.1	$3.6 \times 10^{-4} \pm 1.5 \times 10^{-5}$	[46,48,49]
Fe^{2+}/Fe^{3+} (total)	0.026 ± 0.013	10^{-6}–10^{-2}	$10^{-3} \pm 3.6 \times 10^{-5}$	[48,50,51]

Reference

1. Electrochemical Amino Acid Sensing: A Review on Challenges and Achievements Kaveh Moulaee and Giovanni Neri
2. Arginine--metabolism and functions in the human organis Dorota Scibior 1, Hanna Czeczot
3. Metabolic engineering of microorganisms for the production of L-arginine and its derivatives Jae Ho Shin and Sang Yup Lee
4. 7. Burns, A.; Olszowy, P.; Ciborowski, P. 2—Biomolecules. In Proteomic Profiling and Analytical Chemistry, 2nd ed.; Ciborowski, P., Silberring, J., Eds.; Elsevier: Boston, MA, USA, 2016; pp. 7–24.
5. Joint, F.A.; World Health Organization. Amino Acid Requirements in Human, Food, N, Agriculture Organization of the United, O. World Health, and U. United Nations. In Protein and Amino Acid Requirements in Human Nutrition: Report of a Joint FAO/WHO/UNU Expert Consultation; World Health Organization: Geneva, Switzerland, 2007.
6. Cho, W.; Yoon, Y.; Liu, S.L.; Baek, K.; Sheng, R. Chapter Two—Fluorescence-Based In Situ Quantitative Imaging for Cellular Lipids. In Methods in Enzymology; Gelb, M.H., Ed.; Academic Press: Cambridge, MA, USA, 2017; pp. 19–33.
7. Nur Izzah Ismail, Y.Z.H.-Y.H.; Jamal, P.; Othman, R.; Salleh, H.M. Production of Cysteine: Approaches, Challenges and Potential Solution. Int. J. Biotechnol. Wellness Ind. 2014, 3, 95–101.
8. https://www.webmd.com/vitamins/ai/ingredientmono-1072/glycine#:~:text=Glycine%20is%20an%20amino%20acid,making%20proteins%20in%20the%20body.
9. "Notice of Preliminary Determination of Sales at Less Than Fair Value: Glycine From India" Federal Register 72 (7 November 2007): 62827.
10. https://www.webmd.com/vitamins-and-supplements/glutathione-uses-risks
11. Malathi, M; Thappa, DM (2013). "Systemic skin whitening/lightening agents: what is the evidence?". Indian Journal of Dermatology, Venereology and Leprology. 79 (6): 842–6. doi:10.4103/0378-6323.120752. PMID 24177629.
12. https://www.etslabs.com/library/5#:~:text=The%20Importance%20of%20Glutathione,early%20losses%20of%20aroma%20compounds.

13. Modeling and simulation of carbon nanotube amino-acid sensor: A first-principles study M. Shunaid Parvaiz Khurshed A.Shah H.Alrobeid G.N.Dar Farooq A.Khandaye S.Muzaffar Ali Andrabif Rabia Hamid
14. Carbon Quantum Dots as Fluorescence Nanochemosensors for Selective Detection of Amino Acids Nunzio Tuccitto, Luca Fichera, Roberta Ruffino, Valentina Cantaro, Gianfranco Sfuncia, Giuseppe Nicotra, Giuseppe Trusso Sfrazzetto, Giovanni Li-Destri, Andrea Valenti, Antonino Licciardello, and Alberto Torrisi
15. Carbon dots confined in N-doped carbon as peroxidase-like nanozyme for detection of gastric cancer relevant D-amino acids Zhe Li, Wendong Liu, Pengjuan Ni, Chenghui Zhang, Bo Wang, Guangbin Duan, Chuanxia Chen, Yuanyuan Jiang, Yizhong Lu
16. Hare, D. J.; New, E. J.; de Jonge, M. D.; McColl, G. Imaging Metals in Biology: Balancing Sensitivity, Selectivity and Spatial Resolution. Chem. Soc. Rev. 2015, 44, 5941−5958.
17. Yannone, S. M.; Hartung, S.; Menon, A. L.; Adams, M. W. W.; Tainer, J. A. Metals in Biology: Defining Metalloproteomes. Curr. Opin. Biotechnol. 2012, 23, 89−95.
18. Jarup, L. Hazards of Heavy Metal Contamination. Br. Med. Bull. 2003, 68, 167−182.
19. Ozbek, N.; Baysal, A.; Akman, S. Heavy Metal Determinatıon in Environmental Samples. In Environmental Applications of Instrumental Chemical Analysis; Apple Academic Press: New York, 2015; pp 441−470.
20. Reardan, D. T.; Meares, C. F.; Goodwin, D. A.; McTigue, M.;David, G. S.; Stone, M. R.; Leung, J. P.; Bartholomew, R. M.; Frincke, J. M. Antibodies against Metal Chelates. Nature 1985, 316, 265−268.
21. Cheng, R. P.; Fisher, S. L.; Imperiali, B. Metallopeptide Design: Tuning the Metal Cation Affinities with Unnatural Amino Acids and Peptide Secondary Structure. J. Am. Chem. Soc. 1996, 118, 11349−11356.
22. Wegner, S. V.; Okesli, A.; Chen, P.; He, C. Design of an Emission Ratiometric Biosensor from Merr Family Proteins: A Sensitive and Selective Sensor for Hg2+. J. Am. Chem. Soc. 2007, 129, 3474−3475.
23. Neurobiology: Probing Their Chemistry and Biology with Molecular Imaging. Chem. Rev. 2008, 108, 1517−1549.
24. Nolan, E. M.; Lippard, S. J. Tools and Tactics for the Optical Detection of Mercuric Ion. Chem. Rev. 2008, 108, 3443−3480.

25. Kim, H. N.; Ren, W. X.; Kim, J. S.; Yoon, J. Fluorescent and Colorimetric Sensors for Detection of Lead, Cadmium, and Mercury Ions. Chem. Soc. Rev. 2012, 41, 3210−3244.
26. Jiang, P.; Guo, Z. Fluorescent Detection of Zinc in Biological Systems: Recent Development on the Design of Chemosensors and Biosensors. Coord. Chem. Rev. 2004, 248, 205−229.
27. Yin, J.; Hu, Y.; Yoon, J. Fluorescent Probes and Bioimaging: Alkali Metals, Alkaline Earth Metals and pH. Chem. Soc. Rev. 2015, 44, 4619−44.
28. Hamilton, G. R.; Sahoo, S. K.; Kamila, S.; Singh, N.; Kaur, N.; Hyland, B. W.; Callan, J. F. Optical Probes for the Detection of Protons, and Alkali and Alkaline Earth Metal Cations. Chem. Soc. Rev. 2015, 44, 4415−4432.
29. Carter, K. P.; Young, A. M.; Palmer, A. E. Fluorescent Sensors for Measuring Metal Ions in Living Systems. Chem. Rev. 2014, 114, 4564−601.
30. Sigel, H. Interactions of Metal Ions with Nucleotides and Nucleic Acids and Their Constituents. Chem. Soc. Rev. 1993, 22, 255−267.
31. Navarro, J. A. R.; Lippert, B. Molecular Architecture with Metal Ions, Nucleobases and Other Heterocycles. Coord. Chem. Rev. 1999, 185−186, 653−667.
32. Sigel, R. K.; Sigel, H. A Stability Concept for Metal Ion Coordination to Single-Stranded Nucleic Acids and Affinities of Individual Sites. Acc. Chem. Res. 2010, 43, 974−84.
33. Verma, S.; Mishra, A. K.; Kumar, J. The Many Facets of Adenine: Coordination, Crystal Patterns, and Catalysis. Acc. Chem. Res. 2010, 43, 79−91.
34. Barton, J. K.; Lippard, S. J. Heavy Metal Interactions with Nucleic Acids. In Metal Ions in Biology; Spiro, T. G., Ed.; John Wiley: New York, 1980; pp 31−113.
35. Sherman, S. E.; Lippard, S. J. Structural Aspects of Platinum Anticancer Drug Interactions with DNA. Chem. Rev. 1987, 87, 1153−1181.
36. Ciesiolka, J.; Gorski, J.; Yarus, M. Selection of an RNA Domain That Binds Zn2+. RNA 1995, 1, 538−550.
37. Breaker, R. R.; Joyce, G. F. A DNA Enzyme that Cleaves RNA. Chem. Biol. 1994, 1, 223−9.
38. Grosshans, C. A.; Cech, T. R. Metal Ion Requirements for Sequence-Specific Endoribonuclease Activity of the Tetrahymena Ribozyme. Biochemistry 1989, 28, 6888−6894.

39. Pyle, A. M. Ribozymes: A Distinct Class of Metalloenzymes. Science 1993, 261, 709−714.
40. Ward, W. L.; Plakos, K.; DeRose, V. J. Nucleic Acid Catalysis: Metals, Nucleobases, and Other Cofactors. Chem. Rev. 2014, 114,4318−42.
41. Sigel, R. K.; Pyle, A. M. Alternative Roles for Metal Ions in Enzyme Catalysis and the Implications for Ribozyme Chemistry. Chem. Rev. 2007, 107, 97−113.
42. Greger, R. Central Control of Water and Salt Metabolism. In Comprehensive Human Physiology: From Cellular Mechanisms to Integration; Greger, R., Windhorst, U., Eds.; Springer: Berlin, 1996; pp 1625−1648.
43. Crea, F.; De Stefano, C.; Foti, C.; Lando, G.; Milea, D.; Sammartano, S. Alkali Metal Ion Complexes with Phosphates, Nucleotides, Amino Acids, and Related Ligands of Biological Relevance. Their Properties in Solution. In The Alkali Metal Ions: Their Role for Life; Sigel, A., Sigel, H., Sigel, R. K. O., Eds.; Springer International Publishing: Berlin, 2016; pp 133−166.
44. Foley, K. F.; Boccuzzi, L. Urine Calcium: Laboratory Measurement and Clinical Utility. Lab. Med. 2010, 41, 683−686.
45. Alpoim, M. C. Metal Ions in Biology and Medicine: Les Ions Metalliques En Biologie Et En Medecine; John Libbey Eurotext: Montrouge, France, 2006.
46. Schultze, B.; Lind, P. M.; Larsson, A.; Lind, L. Whole Blood and Serum Concentrations of Metals in a Swedish Population-Based Sample. Scand. J. Clin. Lab. Invest. 2014, 74, 143−148.
47. Fabris, N. Neuroendocrine-Immune Aging: An Integrative View on the Role of Zinc. Ann. N. Y. Acad. Sci. 1994, 719, 353−368.
48. Rodríguez, R. E.; Díaz, R. C. Iron, Copper and Zinc Levels in Urine: Relationship to Various Individual Factors. J. Trace Elem. Med. Biol. 1995, 9, 200−209.
49. Blackburn, N. J.; Yan, N.; Lutsenko, S. Copper in Eukaryotes. In Binding, Transport and Storage of Metal Ions in Biological Cells; The Royal Society of Chemistry: London, 2014; pp 524−555.
50. Lu, L.; Zhang, L.; Li, G. J.; Guo, W.; Liang, W.; Zheng, W. Alteration of Serum Concentrations of Manganese, Iron, Ferritin, and Transferrin Receptor Following Exposure to Welding Fumes among Career Welders. NeuroToxicology 2005, 26, 257−265.
51. Sharp, P. Iron in Eukarya. In Binding, Transport and Storage of Metal Ions in Biological Cells; The Royal Society of Chemistry: London, 2014; pp 282−302.'

Chapter 5

Experimental Process

5.1 Hydrothermal Process

The hydrothermal approach is a quick and easy way to make GQDs [1-4]. GQDs can be created utilizing a range of macromolecular or small molecular substances [5] as the starting materials through high temperature and pressure [6-9]. The principle is to produce GQDs by breaking the bonds between carbon compounds at high temperatures and pressures [10-13].

Tian et al. [14] employed H_2O_2 to manufacture GQDs in an N, N-dimethylformamide (DMF) environment using a one-step solvothermal process. The use of intense sulfuric acid and nitric acid to treat raw materials was fully avoided throughout the preparation process, and no contaminants were added. High-purity GQDs might be achieved without dialysis using evaporation/re-dissolution and filtration. The diameter and thickness of GQDs were found to be primarily dispersed within the ranges of 20-40 nm and 1-1.5 nm, respectively.

Zhang et al. [15] recently manufactured reduced graphene oxide quantum dots (rGOQDs) in 5 hours. They began with graphite to create GO using an enhanced Hummers' process and then used GO and DMF as raw materials for additional hydrothermal treatment in a poly(tetrafluoroethylene) (Teflon)-lined autoclave at 200 °C. The surface doping was nitrogen (N) derived from DMF, and the QY of the produced rGOQDs was 24.62%. They also used rGOQDs to study zebrafish, which provided a helpful reference for the biocompatibility of bio-probes in vivo.

Fig. Hydrothermal autoclave.

5.1.1 Advantages

i. The hydrothermal process can be used to dope a wide range of elements or groups, and the raw ingredients come from a variety of composites [16].
ii. Furthermore, the hydrothermal approach can be used with the chemical oxidation method to produce various GQDs [17-19].

5.1.2 Drawbacks

It has a safety issue because of the high temperature and pressure, and it also takes a long time, usually at least 5 hours [20, 21].

5.2 Preparation of Graphene Oxide

5.2.1 Materials

Graphite flakes (7−10 μm grain size, 99% purity) from Alfa Aesar; sodium nitrate ($NaNO_3$, 99% purity), sulfuric acid (H_2SO_4, 98% by weight, G.R.), potassium permanganate ($KMnO_4$, 99% purity), hydrochloric acid (HCl), hydrogen peroxide (H_2O_2, 30% by weight, A.R.) from Merck were used for synthesis. The deionized water was taken from a Direct-Q Millipore deionized (18 Ω at 25°C).

5.2.2 Preparation

i. The oxidation and exfoliation of graphite flakes using Hummer's method produced graphene oxide (GO). To begin the process, 3 grams of graphite powder and 3 grams of sodium nitrate were mixed well and placed in a 500 ml beaker containing 180 grams of concentrated sulfuric acid. This solution was stirred continuously for two hours.
ii. As a next step, 10 gm of potassium permanganate was added slowly to the black solution for 30 minutes at a temperature of 15°C or less. For the next 24 hours, the mixture was stirred vigorously.
iii. In order to change the colour from black to golden yellow, 200 mL DI and 10 mL 30% H2O2 were gradually added to the solution while maintaining a temperature of 40°C. Afterwards, the mixture was allowed to cool to room temperature and settle.

iv. The clear supernatant was decanted, centrifuged twice at 12000 rpm for 15 minutes, washed once with 5% hydrochloric acid, and the supernatant was removed.

v. Followed by a DI wash, the bottom portion (brown in colour) of the centrifuged tube was centrifuged for 10 minutes at 12000 rpm to generate three layers. After removing the upper colourless component, the centre light brown solution was separated.

vi. The bottom section of the solution containing GO and excess graphite was centrifuged 5 times, with the middle portion containing GO retrieved and the lower portion removed each time.

vii. The light brown suspension was dried in a vacuum oven at 48°C for 24 hours to yield freshly manufactured GO.

5.3 Synthesis of GQD & NGQD

The GQD and NGQD used in this study were prepared using a hydrothermal, sonication, and purifying procedure.

Materials required are previously prepared Graphene Oxide, Imidazole (≥99% (titration), crystalline) by Sigma Aldrich and Ammonia.

5.3.1 Normal Synthesis of NGQD

Initially, 15 mg of Graphene Oxide was mixed with 50 ml of de-ionized water before being sonicated for 15-20 minutes till the Graphene Oxide was mixed and the solution turned blackish. 10 mg Imidazole was sonicated for 2-3 minutes in 10 ml de-ionized water. The Graphene oxide solution and Imidazole solution were then combined in a beaker to generate a fresh solution, to which 10 ml of Ammonia was added. The solution was stored in a Teflon autoclave, which was firmly packed with Teflon tape and then covered with a steel jacket. The experiment was carried out for 6, 12, 18, 24, and 30 hours in an oven set at 90 degrees Celsius. We obtain impure Nitrogen-doped Graphene Quantum Dots (NGQD) at the end of the process.

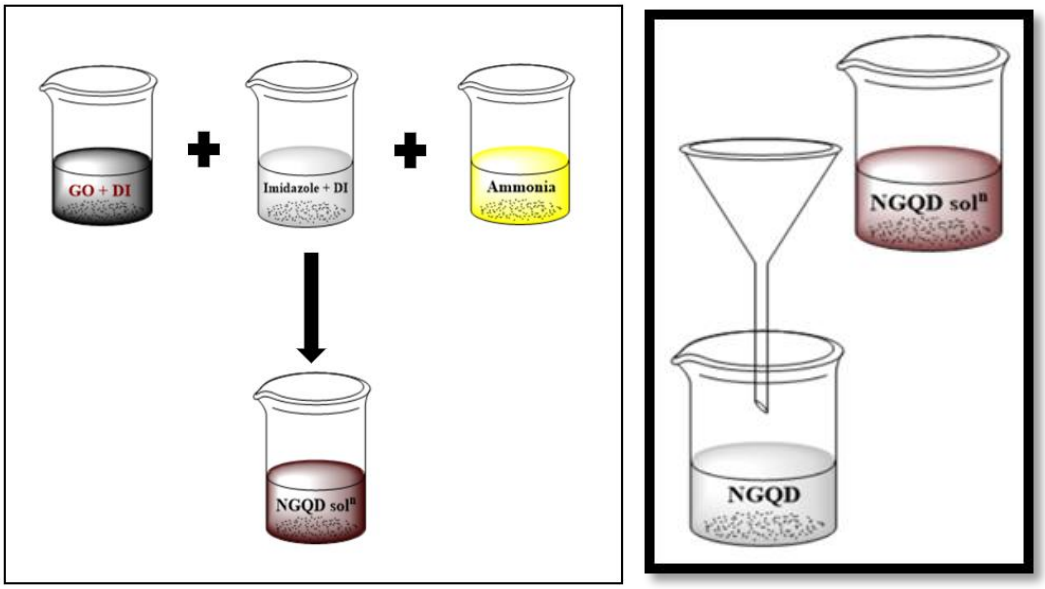

Fig. Preparation of NGQD.

5.3.1.1 Purification of NGQD

Impure Nitrogen-doped Graphene Quantum Dot solution was poured through a conical flask with filter paper, and a considerable portion of the pure solution was collected in a beaker placed beneath the conical flask. The solution was stored in a beaker and a bid was placed in the middle of the beaker, heat and magnetic stirring were applied simultaneously with the help of a magnetic stirrer until the pH of the solution was decreased to 6.5, which was initially approximately 12. The polymers in the solution are removed by osmosis, the NGQD solution is kept in the dialysis tube and both ends are tied with a rubber band, it is kept within a beaker containing de-ionized water, and the tube is completely immersed in the de-ionized water.

Products are NGQD6, NGQD12, NGQD18, NGQD24 & NGQD30.

5.3.2 Control synthesis of GQD

To commence, 15 mg of Graphene Oxide was mixed with 70 ml of de-ionized water before being sonicated for 15-20 minutes to mix the Graphene Oxide and darken the solution. The solution was maintained in a Teflon autoclave encased in a steel jacket and securely sealed with Teflon tape. The experiment was conducted in a 90-degree Celsius oven for 6, 12, 18, 24, and 30 hours.

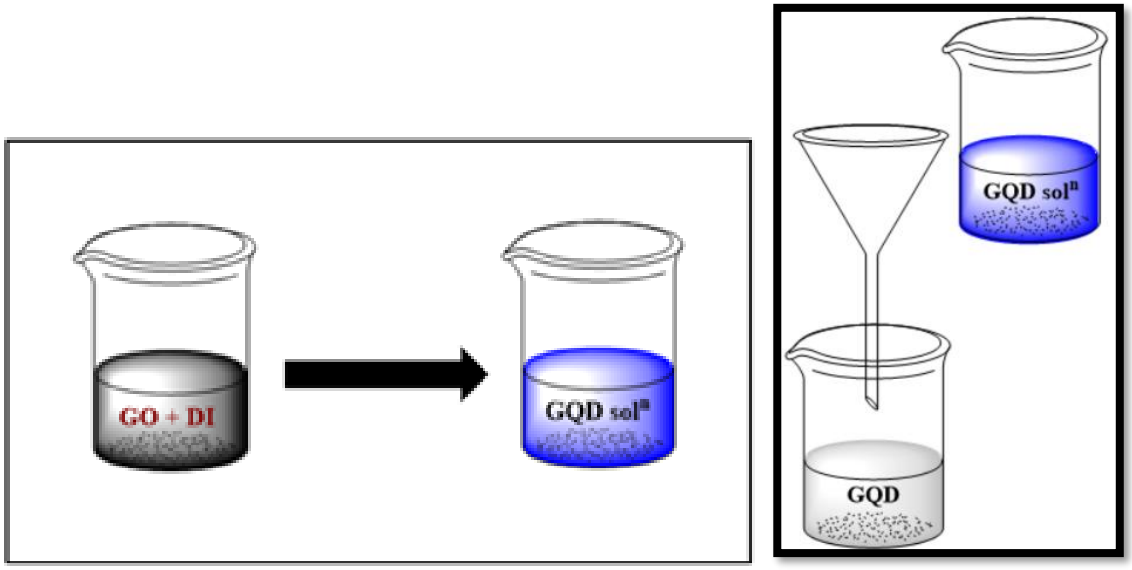

Fig. Preparation of GQD.

5.3.2.1 Purification of GQD

A portion of the pure Graphene Quantum Dot solution was collected in a beaker placed beneath the conical flask after the impure solution was passed through it with filter paper.

Products are GQD6, GQD12, GQD18, GQD24 & GQD 30.

Reference

1. Liu B, Xie J, Ma H, Zhang X, Pan Y, Lv J, Ge H, Ren N, Su H, Xie X, et al. From graphite to graphene oxide and graphene oxide quantum dots. Small. 2017;13:1601001.
2. Teymourinia H, Salavati-Niasari M, Amiri O, Farangi M. Facile synthesis of graphene quantum dots from corn powder and their application as down conversion effect in quantum dot-dye-sensitized solar cell. J Mol Liq. 2018;251:267–72.
3. Chu X, Dai P, Dong Y, Sun W, Bai L, Zhang W. The acetic acid gas sensing properties of graphene quantum dots (GQDs)–ZnO nanocomposites prepared by hydrothermal method. J Mater Sci: Mater Electron. 2017;28:19164–73.
4. Chu X, Dai P, Liang S, Bhattacharya A, Dong Y, Epifani M. The acetone sensing properties of ZnFe2O4-graphene quantum dots (GQDs) nanocomposites at room temperature. Phys E. 2019;106:326–33.
5. Mehrdad-Vahdati B, Pourhashem S, Sedghi M, Vaezi Z, Shojaedin-Givi B, Rashidi A, Naderi-Manesh H. A novel aspect of functionalized graphene quantum dots in cytotoxicity studies. Toxicol In Vitro. 2019;61:104649.
6. Wang L, Li W, Wu B, Li Z, Wang S, Liu Y, Pan D, Wu M. Facile synthesis of fluorescent graphene quantum dots from coffee grounds for bioimaging and sensing. Chem Eng J. 2016;300:75–82.
7. Wang Y, Jin Y, Duan Y, Jia M. Fe3O4 quantum dots on 3D-framed graphene aerogel as an advanced anode material in lithium-ion batteries. Ionics. 2017;23:2005–111.
8. Gao XX, Zhou X, Ma YF, Wang CP, Chu FX. A fluorometric and colorimetric dual-mode sensor based on nitrogen and iron co-doped graphene quantum dots for detection of ferric ions in biological fluids and cellular imaging. New J Chem. 2018;42:14751–6.
9. Mathew MS, Sukumaran K, Joseph K. Graphene carbon dot assisted sustainable synthesis of gold quantum cluster for bio-friendly white light emitting material and ratiometric sensing of mercury (Hg2+). ChemistrySelect. 2018;3:9545–54.
10. Wang L, Wu B, Li W, Wang S, Li Z, Li M, Pan D, Wu M. Amphiphilic graphene quantum dots as self-targeted fluorescence probes for cell nucleus imaging. Adv Biosyst. 2018;2:1700191.
11. Huang D, Zeng M, Wang L, Zhang L, Cheng Z. Biomimetic colloidal photonic crystals by coassembly of polystyrene nanoparticles and graphene quantum dots. RSC Adv. 2018;8:34839–47.
12. Pourhashem S, Ghasemy E, Rashidi A, Vaezi MR. Corrosion protection properties of novel epoxy nanocomposite coatings containing silane functionalized graphene quantum dots. J Alloy Compd. 2018;731:1112–8.
13. Oh B, Lee CH. Development of thiolated-graphene quantum dots for regulation of ROS in macrophages. Pharm Res. 2016;33:2736–47.
14. Tian R, Zhong S, Wu J, Jiang W, Shen Y, Jiang W, Wang T. Solvothermal method to prepare graphene quantum dots by hydrogen peroxide. Opt Mater. 2016;60:204–8.
15. Zhang JH, Sun T, Niu A, Tang YM, Deng S, Luo W, Xu Q, Wei D, Pei DS. Perturbation effect of reduced graphene oxide quantum dots (rGOQDs) on aryl hydrocarbon receptor (AhR) pathway in zebrafish. Biomaterials. 2017;133:49–59.

16. Das R, Rajender G, Giri PK. Anomalous fluorescence enhancement and fluorescence quenching of graphene quantum dots by single walled carbon nanotubes. Phys Chem Chem Phys. 2018;20:4527–37.
17. Wang S, Li Z, Xu X, Zhang G, Li Y, Peng Q. Amino-functionalized graphene quantum dots as cathode interlayer for efficient organic solar cells: quantum dot size on interfacial modification ability and photovoltaic performance. Adv Mater Interfaces. 2019;6:1801480.
18. Wang R, Fan H, Jiang W, Ni G, Qu S. Amino-functionalized graphene quantum dots prepared using high-softening point asphalt and their application in Fe3+ detection. Appl Surf Sci. 2019;467–468:446–55.
19. Xu H, Zhou S, Liu J, Wei Y. Nanospace-confined preparation of uniform nitrogen-doped graphene quantum dots for highly selective fluorescence dual-function determination of Fe3+ and ascorbic acid. RSC Adv. 2018;8:5500–8.
20. Luo Y, Li M, Sun L, Xu Y, Hu G, Tang T, Wen J, Li X. Tuning the photoluminescence of graphene quantum dots by co-doping of nitrogen and sulfur. J Nanopart Res. 2017;19:1328.
21. Fang X, Ding J, Yuan N, Sun P, Lv M, Ding G, Zhu C. Graphene quantum dot incorporated perovskite films: passivating grain boundaries and facilitating electron extraction. Phys Chem Chem Phys. 2017;19:6057–63.

Chapter 6

Instruments

&

Apparatus

6.1 Photoluminescence Spectroscopy (PL)

6.1.1 Introduction

Photoluminescence (PL) spectroscopy is a simple and direct, non-destructive method. By using this method, you can determine a material's band gap, impurity level, defect detection, recombination mechanism, surface structure, fluorescence property, and its excited states. Photoluminescence spectroscopy is performed in the non-contact mode. It is a non-destructive method of examining a material's electronic structure. In simple terms, it is an instrument that interacts with light and matter.

6.1.2 Basic Principle

When light strikes a sample, the excess energy is absorbed by the material. This is referred to as photo-excitation. One method by which the sample dissipates this excess energy is light emission, also known as luminescence. Photoluminescence is defined as luminescence caused by photo-excitation. When a material is excited, the electrons in the material occupy the allowed excited states. To return to their stable, i.e., equilibrium or ground state, these excited electrons dissipate the excess energy in the form of light (radiative process) or any non-radiative process. The energy difference between the two electronic states involved in the transition between excited and equilibrium states is proportional to the emitted light energy (photoluminescence). The proportion of the radiative process determines the amount of light emitted.

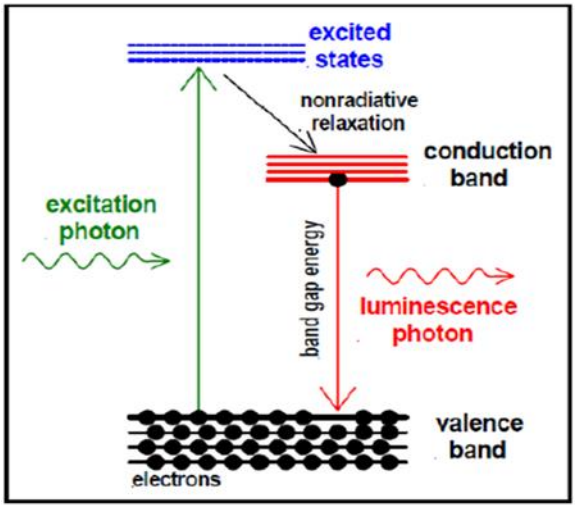

6.1.3 Photoluminescence Different Modes

• **Resonant radiation:** A specific wavelength photon is absorbed in this process, accompanied by the instantaneous emission of an equivalent photon. This process has no discernible internal energy transitions between absorption and emission, and the time scales are on the order of 10 nanoseconds.

• **Fluorescence:** When the chemical substrate initiates the internal energy transition by emitting photons before restoring to its ground state, a certain joule of absorbed energy is liberated, resulting in the emitted light having less energy than the absorbed. One of the known mechanisms with a lifetime of 10^{-8} to 10^{-4} s is fluorescence.

• **Phosphorescence:** It is a radiation-based transition in which the absorbed energy undergoes an electronic transition with multiple spin states, i.e., intersystem crossing (ISC). The lifespan of the phosphorescence phenomenon is typically 10^{-4} - 10^{-2} s, which is significantly longer than the Fluorescence lifespan. Thus, phosphorescence occurs less frequently than fluorescence because the molecule in its triplet state has a greater chance of experiencing intersystem crossing to a lower energy state prior to the occurrence of phosphorescence.

6.1.4 Spectroscopy

When light is focused on the material, electrons within it can migrate into permitted excited states. When these electrons return to their equilibrium states, the excess energy is released, which may or may not involve the emission of light (a radiative process) (a non-radiative process). The energy of the produced light is determined by the difference in energy levels between the two electron states involved in the transition between the excited state and the equilibrium state (photoluminescence). The amount of light emitted is proportional to the proportionate contribution of the radiative process. In most cases, the released light has a longer wavelength than the absorbed radiation and thus contains less energy.

When the absorbed electromagnetic radiation is sufficiently strong, one electron can absorb two photons, resulting in the emission of light with a shorter wavelength than the absorbed energy. When the released radiation has the same wavelength as the absorbed light, resonance fluorescence occurs. Photoluminescence occurs when radiation is absorbed in the ultraviolet part of the spectrum, which is invisible to the human eye, and the released light is in the visible

range. S_0 is the ground state of a fluorophore (fluorescent molecule), while S_1 is the first (electronically) excited state. S_1 is a molecule that can relax in several ways.

It can undergo non-radiative relaxation, in which the excitation energy is transferred to the solvent as heat (vibrations). Excited organic molecules can also relax by converting to a triplet state, which can then relax via phosphorescence or a secondary nonradiative relaxation process. An S_1 state can also relax as a result of interaction with a second molecule via fluorescence quenching. Molecular oxygen (O_2) is a highly effective fluorescence quencher due to its unique triplet ground state.

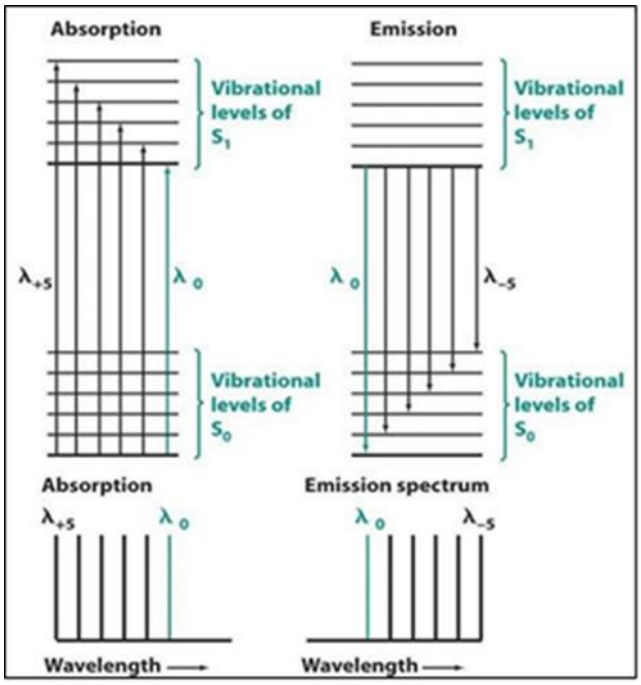

Figure: Representing the energy-level diagrams which mention why structure is seen in the absorption as well as emission spectrum and also why the spectra are roughly mirrored images of each other.

6.1.5 Relation between Absorption and Emission Spectrum

Fluorescence and phosphorescence are more likely at lower energies than absorption (the energy of excitation). In the case of absorption, λ_0 wavelength denotes the transition from the ground state of vibration, i.e., S_0 to S_1. When S_1 molecules are excited vibrationally, they move to a lower vibrational level before emitting radiation. At λ_0 wavelength, a very high cascade of peaks occurs at a higher wavelength. Both the emission and absorption spectra are likely to

have a mirror image relationship if the spacing of vibrational levels is roughly equivalent and the probability of transition is similar. λ_0 transitions do not completely overlap.

In addition to solvation, a radiation-absorbing molecule that is mostly in its ground state, S_0; has a solid geometry. Transitions between electronic states are quicker than atoms' vibrational movement or solvent molecules' translational movement; once the radiation is absorbed, the S_1 stimulated molecule retains its geometry and solvation S_0 state.

Geometry and solvation are both altered to the greatest extent possible soon after stimulation. This rearrangement reduces the excited molecule's energy. When an S_1 molecule fluoresces, it returns to its original S_0 shape and solvation. This unbalanced configuration must have more energy than an S_0 molecule with S_0 geometry and solvation. The net result is depicted in the Figure, where the excitation energy exceeds the emission energy.

6.1.6 Instrumentation of Photoluminescence

A spectrofluorometer is an analytical equipment that records and measures the fluorescence of a sample. To record the fluorescence, the excitation, emission, or both wavelengths are scanned. The investigation of signal deviation with regard to time, temperature, concentration, polarisation, or other variables is studied using extra attachments.

The fluorescence spectrometer's block diagram is shown below. Fluorescence spectrometers use monochromators (wavelength selectors), laser sources (sample illumination), detectors, and corrected spectrums.

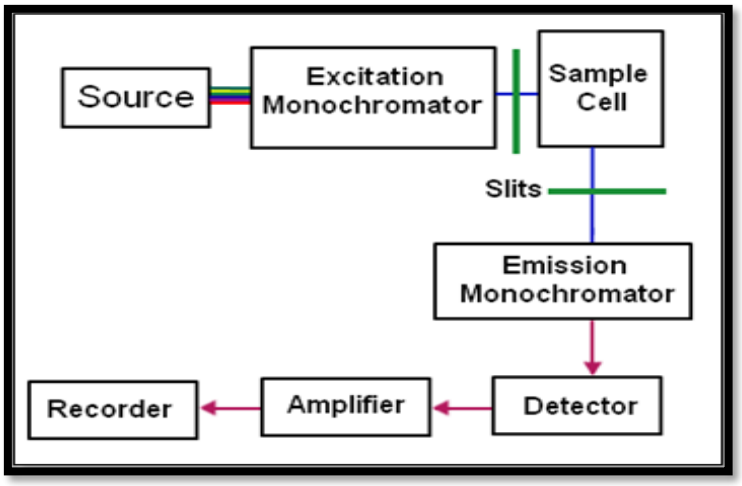

• **Source of Illumination:**

A continuous type, 150 W ozone-free xenon arc lamp is used as the light source. The light from the lamps is collected by a diamond-turned elliptical-shaped mirror, which is then directed into the entry slit of the excitation monochromators.

A quartz-based window is utilised to segregate the excitation monochromator from the lamp's housing, which vents heat out of the device and protects against the lamp's rare failure. The ability to resolve the entire spectrum stretches and decreases spherical aberrations and re-diffraction.

• **Monochromators:**

Monochromators are classified into two types: excitation monochromators and emission monochromators. It employs whole reflective optics to maintain high resolution across the entire spectrum while also reducing aberrations (spherical) and re-diffraction.

• **Gratings:**

Reflection Grating is an essential component of a monochromator, whose aim is to scatter striking (incident) light through vertically positioned grooves. Spectra are obtained by rotating gratings with 1200 grooves per mm and being blazed at 330 nm (excitation) at 500 nm (emission). The grating is coated with a protective coating of MgF_2 to prevent oxidation.

• **Slits:**

At the monochromator's entrance and exit sites, very flexible slits are used. The incident light's bandpass is defined by the width of the slit on the excitation monochromator, whilst the fluorescence intensity signal is controlled (recorded by the signal detector) by the slits on the emission monochromator.

When determining slit width, the trade-off is signal strength versus spectral resolution. When the slit width is greater, the resolution decreases because more light falls on the sample as well as the detector, but when narrower slits are employed, the resolution increases but at the expense of the signal.

• **Shutters:**

An excitation shutter is installed beneath the exit slit of the excitation monochromator to protect the sample from photobleaching or photodegradation caused by prolonged exposure to light.

The detector is shielded from the bright light by an emission shutter located just before the entry of the emission monochromator.

• **Sample compartment:**

Several alternative attachments and fibre optic bundles are included in the sample compartment to transport the excitation beam to the remote sample and return the emission beam to the emission monochromator.

• **Detectors:**

There are two sorts of detectors: signal detectors and reference detectors. The photon counting signal detector is an R928P photomultiplier tube that directs the signal to a photon counting module. The objective of the reference detector is to monitor the xenon lamp for wavelength and time-dependent output adjustment. This detector is based on UV, which increases the silicon photodiode, which is situated just before the sample compartment.

Figure: Horiba Jobin Yvon Fluromax spectrofluorometer

6.1.7 Photoluminescence Spectroscopy Limitations

Despite the fact that it is not a qualitative technique, it can be used to identify tiny concentrations of optical centres. The main scientific PL constraint is that some optical centres

may have a large number of excited states that are not occupied at low temperatures. Another significant drawback of PL is the disappearance of the luminous signal.

6.1.8 Applications

• Determination of Band gap:

In semiconductors with radiative transitions, the band gap denotes the energy difference between the conduction band (top) and the valence band (bottom). The range of a semiconductor's PL spectrum is utilised for non-destructive bandgap analysis. This mode allows you to quantify the composition of the elements in a semiconductor compound as well as material specifications that influence device efficacy, such as solar cells.

• Identification of level of Impurity as well as a defect:

When the radiative transition happens in semiconductors, some localised defect levels are induced. The photoluminescence energy can identify specific flaws associated with these levels, whereas the PL quantity can determine their concentration. The photoluminescence spectra of the sample at low temperatures frequently display spectrum peaks associated with impurities existing inside the host material. Highly sensitive Fourier transform photoluminescence microspectroscopy has the potential to detect very minute amounts of planned and unexpected impurities, which have a significant impact on material quality and device performance.

• Recombination phenomena:

Both radiation and non-radiation processes involve the "recombination" mechanism (Return to equilibrium). The amount of PL material emitted is directly related to the relative amount of radiative and nonradiative recombination rates.

The amount of PL and impurities is typically associated with nonradiative rates, and it is reliant on the photo-excitation intensity as well as temperature, both of which are directly related to the dominant recombination mechanism. As a result, qualitative PL analysis includes tracking changes in material quality as a function of variables such as growth and processing, which aids in understanding the fundamental physics of the recombination mechanism.

• Surface structure and excited states:

Some widely used conventional methods, such as XRD, IR, and Raman spectroscopy, are frequently insensitive to oxide-supported catalysts with low metal oxide concentrations. Because PL is overly sensitive to surface effects or semiconductor-based particle adsorbed species, it is used as a probe of electron-hole surface processes.

Figure: Photoluminescence analysis carried out by Horiba Jobin Yvon Fluromax spectrofluorometer

6.2 Diffuse Reflectance Spectroscopy (DRS)

6.2.1. UV-Vis Near-Infrared Spectroscopy:

UV-Visible near-infrared (UV-Vis-NIR) In the ultraviolet-visible spectral region, a spectrophotometer measures optical transmittance, absorbance, and reflectance. Optical transmittance, absorbance, and reflectance in the ultraviolet-visible spectral range are measured using a UV-Vis near Infrared (UV-Vis-NIR) Spectrophotometer.

The percentage of the radiation absorbed, transmitted, or reflected at each wavelength is measured using UV-VIS absorption spectroscopy. Typically, this is achieved by scanning the wavelength range and measuring absorption. It is commonly used in organic chemistry to study

the extent of multiple bonds or aromatic conjugation inside molecules. The technique can be extended to gases and solids, as well as beyond absorption to detect reflected light rather than transmitted light.

Light absorption can be described by two fundamental laws:

- **Lambert's Law -** The proportion of incident light absorbed by a transparent medium is independent of the intensity of the light (provided that there is no other physical or chemical change to the medium). Therefore, successive layers of equal thickness will transmit an equal proportion of the incident energy.

Lambert's law can be expressed by: $\mathbf{\frac{I}{I_0} = T}$

Where I is defined as the intensity of the transmitted light, I_0 is the intensity of the incident light, and T is the Transmittance.

- **Beer's Law -** The absorption of light is directly proportional to both the concentration of the absorbing medium and the thickness of the medium in the light path.

A combination of the two laws (known jointly as the Beer-Lambert Law) defines the relationship between absorbance () and transmittance ().

$$\mathbf{A = \log\frac{I_0}{I} = \log\frac{100}{T} = \varepsilon cb}$$

Where, is absorbance (no unit of measurement), molar absorptivity ($dm^3mol^{-1}cm^{-1}$), molar concentration (mol dm^{-3}), and path length (cm).

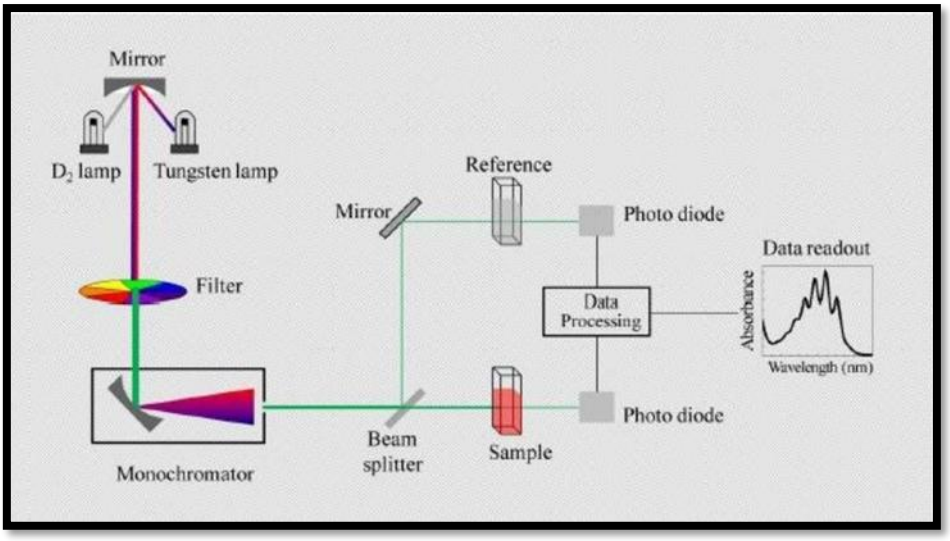

Figure: Basic Principles of UV-VIS Spectroscopy

6.2.2 Light Reflection and Reflectance Spectra:

The spectrometer beam is directed into the sample and reflected, dispersed, and transmitted, resulting in diffuse reflectance (shown on the right). The accessory catches and directs back reflected, diffusely scattered light to the detector optics (part of which is absorbed by the sample). Diffuse reflection refers to the portion of a beam that is scattered within a sample and returns to-

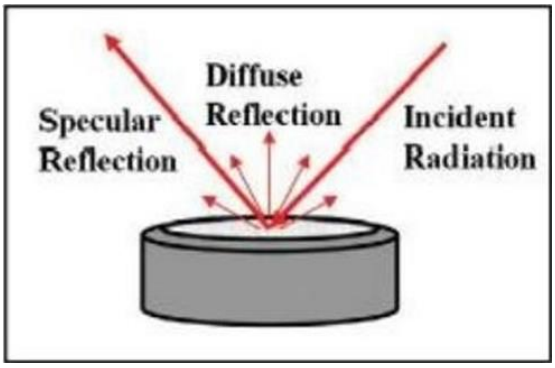

Figure: Diffuse and Specular Reflectance

Other characteristics that contribute to great spectral quality in diffuse reflectance sampling include particle size, refractive index, homogeneity, and packing. Despite all of these sample preparation processes, the raw diffuse reflectance spectra will appear different from their transmission counterpart (stronger than expected absorption from weak IR bands).

To correct these discrepancies, a Kubelka-Munk conversion can be performed to a diffuse reflectance spectrum.

Kubelka-Munk Function: $\mathbf{F = \frac{(1-R)^2}{R} = \frac{k}{S}}$

R stands for the sampled layer's absolute reflectance, k for the molar absorption coefficient, and s for the scattering coefficient.

The spectrum above depicts the spectral conversion of ibuprofen acquired using diffuse reflectance.

The Kubelka-Munk transformed spectrum for ibuprofen compares well to the transmission spectrum and is readily detected using a transmission spectral database library search.

Diffuse reflectance spectroscopy (DRS) of (nanoscaled) powders is a frequently used and powerful instrument in material sciences and industry. An input light beam's scattered intensity

is scanned over the sample as a function of wavelength, and the resulting data set is analysed in terms of macroscopic optical properties such as total reflectivity.

Furthermore, DRS has the capacity to detect particle absorption characteristics even at sub-micron length scales. Absolute values of the absorption coefficient, as well as dispersive qualities, are crucial for a variety of materials with strong commercial potentials, such as pigments or phosphors. Absorption qualities influence the macroscopic optical properties of dielectric powders, but they also influence the losses of internally emitted light.

As a result, DRS is routinely utilised in applications that fall short of its capabilities, and it is mostly used to determine macroscopic optical properties. The purpose of this study is to provide end-to-end guidance from sample preparation to absorption spectra determination by tackling the tough challenge of optical characterization of pure, dielectric (nano-)powders.

The introduction of a new powder pellet preparation technique that enables for the manufacture of samples with excellent Lambertian scattering behaviour that are also highly reproducible is highlighted. As a result, thick, non-translucent samples are used to enable dependable experimental access to diffuse reflectance spectroscopy and subsequent absorption coefficient determination.

This method offers various advantages, including

1) high-quality reflectance spectra,

2) good consistency in calculating absorption features, and

3) easy identification of signal artefacts, allowing for further reduction.

6.2.3 Measurement Setup:

6.2.3. (a) Requirements and Procedures

A specialised optical setup is necessary for reliable and reproducible measurements of diffuse reflectance spectra. While it is possible to create it from scratch and acquire satisfactory results, numerous dedicated spectrometers for greater precision measurements are commercially available at the time of writing this research. Naturally, successor or previous models are also appropriate, depending on their characteristics and measurement choices.

6.2.3. (b) Components of Diffuse Reflectance Spectrophotometer

A spectrophotometer consists of the following components

- A source of radiation of appropriate wavelengths
- Monochromator and optical geometry
- Filter Sample compartment
- Detector, Photomultiplier, Measuring system, Computer

Because double-beam spectrometers simultaneously detect the sample and the white standard, calculating the diffuse reflectance of non-luminescent substances is straightforward, fast, and precise. Because of the parallel acquisition process, lamp intensity changes are not a concern.

Extraneous light emission at wavelengths other than the excitation wavelength generates erroneous extra signals in fluorescence, rendering an unfiltered diffuse reflectance spectrum incorrect. Using a fluorescence spectrometer, on the other hand, gives you the distinct advantage of being able to readily do diffuse reflectance measurements on any material.

Such a scenario is now omitted in favour of a collimated (or, optionally, defocused) beam. For fluorescent samples, a configuration with two independent monochromators is required: The excitation monochromator selects a wavelength for sample illumination, while the emission monochromator transmits the linear diffuse reflectance of the sample, cancelling any further fluorescence emission.

Figure: UV-VIS-NIS (SHIMADZU UV-3600) Spectrophotometer

As a result, this mode of operation, in which both monochromators are set to the same wavelength, is generally referred to as synchronous scanning. In addition to monochromators, additional spectral filters remove potential higher diffraction orders transmitted by grating-based monochromators, as well as sample fluorescence. If only monochromatic illumination is required, the light source/monochromator combination can be replaced by a suitable laser or bandpass filtering behind a broadband emission source.

If intensity fluctuations are a significant problem, such as due to lamp power drifts or ambient temperature changes, it is advisable to separate a small amount of the excitation light into a low-drift reference detector. The remainder of the material will be used to illuminate the samples. The reference detector's signal can then be utilised to scale the measured diffuse reflectance intensities. Any extra detector, however, will eventually increase overall electronic noise and should so be utilised with prudence.

When compared to vertically placed samples, which are common in integrating spheres where an additional cover window is frequently used to keep the powder in place, horizontal alignment of the powder sample has the distinct advantage of eliminating potential spectrometer contamination due to material gliding off of the (brittle) surface.

Even without a cover window, the horizontal alignment ensures that the sample is preserved throughout the measurement and that contamination of its surroundings is avoided. A parallel excitation/emission beam geometry also eliminates specular reflection losses caused by a slight tilt of the incident light direction relative to the sample surface normal. This significantly reduces the impact of sample surfaces that aren't perfectly Lambertian. The beam path requires at least one additional mirror to reflect the excitation beam downwards onto the sample to account for this geometry. This mirror also relays the emission beam towards the detection arm in an optimised setup.

The sample's diffusely reflected light is directed into the optical detection path and then recorded by a detector within the spectrometer, such as a photomultiplier tube (PMT). We'll stick to single-channel detection for the sake of simplicity.

6.2.4 White Standards

Experimenting with precise, absolute values for diffuse reflectance of a sample is difficult in general. It invariably necessitates a thorough understanding of the used spectrometer,

particularly its optical transfer function. The use of reference materials with well-documented diffuse reflectance is a common method for investigating the peculiarities of spectrometers and for calibration purposes. The diffuse reflectance of such white standards is characteristic over a wide spectral range.

From both the diffuse intensity signal of sample Is and the white standard Iws, the diffuse reflectance R = Is/Iws is calculated. Historically, white standard materials have been micro- and nano-scaled powders of magnesium oxide (MgO) and barium sulphate ($BaSO_4$), which have a pronounced and spectrally homogeneous diffuse reflectance in the visible spectrum.

Following that, a typical three-fold scan would consist of:

1. Determine the white standard.

2. Take a sample and measure it.

3. Determine the white standard.

6.3 Surface Analysis

6.3.1 X-Ray Photoelectron Spectroscopy

X-Ray Photoelectron Spectroscopy is one of the most powerful surface analytical techniques capable to provide accurate qualitative elemental analysis (for all elements except hydrogen and helium), quantitative composition and determination of chemical states such as binding and oxidation can also be done. The information should be originated within ~10 nm from the outer surface.

6.3.1.1 Principles of XPS

XPS is based on the photoelectric effect which is discovered by Hertz in 1887. In this case, electron emission from the surface is resulted due to the interaction of an x-ray photon of sufficient energy with the solid surface. The applied x-ray of 1-15 KeV energy is capable to induce electrons not only from the outer shells but also from the core levels of all elements of periodic table. The governing equation of this phenomenon is as follows:

$$h\nu = E_b + E_{kin} + W_f$$

Where E_b is binding energy, E_{kin} is the kinetic energy of the photoelectron, W_f is the work function of the instrument.

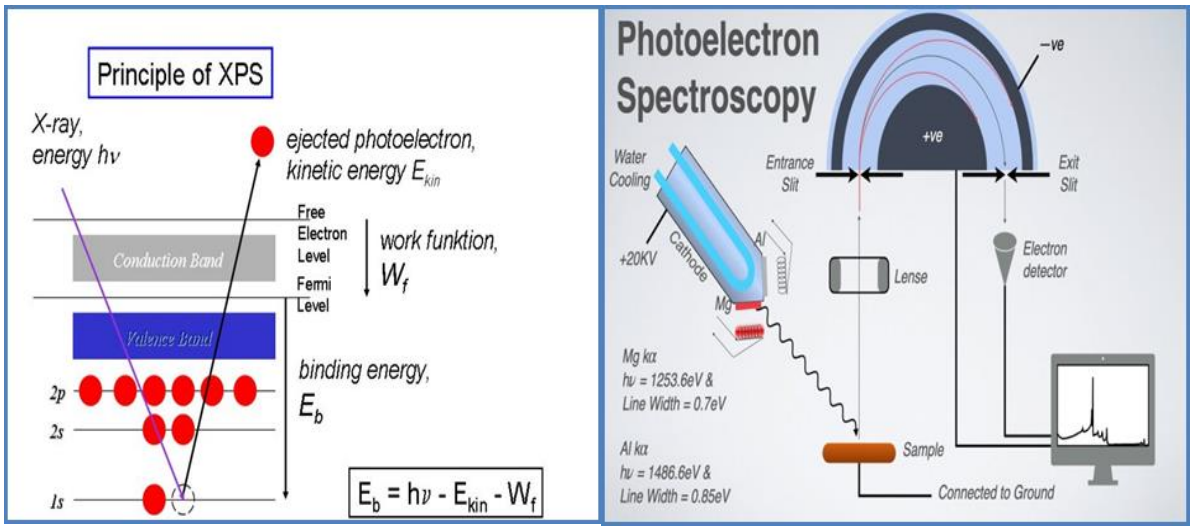

Fig. Basic principles and constructions of XPS.

6.3.1.2 Configuration of XPS instrument

The experimental set-up contains mainly the following parts: (i) an X-ray source for XPS, (ii) an electron energy analyzer, combined with a detection system, and (iii) a sample stage, all contained within a vacuum chamber. As for most techniques, the system is operated and controlled by a computer, usually provided a software allowing mathematical treatment.

- **X-ray source**

Since XPS is concerned with the analysis of core electrons from a solid surface, sources used in XPS must be able to produce photons of sufficient energy to access a suitable number of core electron levels. Photons of this energy lie within the X-ray region of the electromagnetic spectrum. As a result, these are otherwise referred to as X-rays. X-ray tubes produce X-rays by directing a sufficiently energetic electron beam at some metallic solid. This metallic object is referred to as the X-ray anode, with the electron source being the cathode. Although any solid can in principle is used as an X-ray anode, Al has become the most commonly used in XPS

due to the relatively high energy and intensity of Al-Kα X-rays, the minimal energy spread of Al-Kα X-rays and the fact that Al is an effective heat conductor.

- **Electron energy analyzer**

Since the information in XPS is derived from the Ekin of the electron emissions, effective analysis requires an energy filter that exhibits both a high-energy resolution and a high transmission. The former allows for the separation of closely spaced peaks, thereby optimizing speciation identification capabilities, while the latter allows for sensitivity to be maximized. The two primary energy filter configurations used in XPS named Cylindrical Mirror Analyzer (CMA), and Concentric Hemispherical Analyzer (CHA).

- **Detector**

In XPS, it is not only important to measure the energy of the electron emissions but also the number of electrons produced. XPS spectra are plotted in units of energy versus intensity, with the energy defined by the energy analyzer used and the intensity defined by the number of electrons recorded by the detector. To obtain the best possible sensitivity, the detector must be capable of recording individual electrons, that is, operating in pulse counting mode. This signal is recorded in units of current (A), which are then represented in units of counts per second.

- **Sample stage**

The mounting of the samples on the sample holder should be done in such a way that electrical conduction is guaranteed. This is achieved by using metallic clips or bolt-down assemblies. Alternatively, metal-loaded tape may also be used. In the case of powders, the particles can be pressed into an indium foil or carbon tape.

- **Vacuum requirement**

As XPS is a surface-sensitive method, impurities can play a major role in the observed spectra. The criterion is that a good vacuum is needed to maintain the integrity of the surface. In general, 10-5Torr is sufficient to allow the Photoelectron to reach the detector without suffering collisions with other gas molecules. On the other hand, 10-9Torr or lower is required to keep an active surface clean for more than several minutes. So, 10-8 - 10-9Torr provides a reasonable

pressure range for XPS measurement. Sample analysis was performed on the SPECS with a hemispherical energy analyzer (HAS 3500). Photoelectrons were excited using the monochromatic Mg Kα X-ray (1253.6eV) or Al Kα X-ray (1486.6eV) was used as the excitation source operated at 10 kV and with an anode current 17 mA.

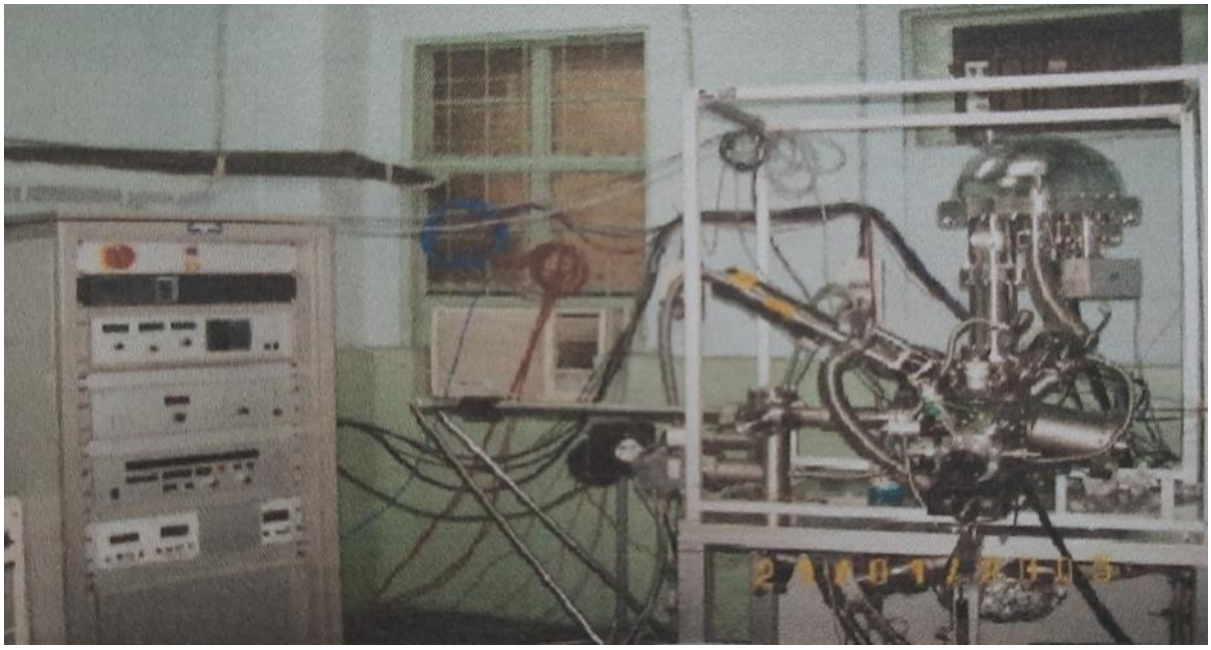

Fig. Experimental set up of XPS.

Chapter 7

Results

&

Discussions

7.1 Optical Analysis

Photoluminescence and UV-vis spectra were used to evaluate the optical characteristics. GQDs exhibit unusual absorption and luminescence characteristics due to their simple capture nature and look. GQDs are usually expressed as a significant absorption peak in the deep UV region caused by the p-p* transition. At a higher wavelength, the tiny absorption peaks associated with the n-p* transition may also be seen. The graphene core and indefinite chemical groups are held together on the surface of GQDs, and so the photoluminescence is organized by the graphene core and neighbouring chemical groups [1]. GQDs' basic qualities are mostly determined by their form, size, and edge structure, and they play an active role in the location of absorption peaks.

7.1.1 Bandgap Analysis

E_g^{opt} = 1240 nm/λ_{onset} was used to compute the optical bandgap from the onset wavelength of absorption, where E_g^{opt} is the optical bandgap and λ_{onset} is the onset wavelength of absorption.

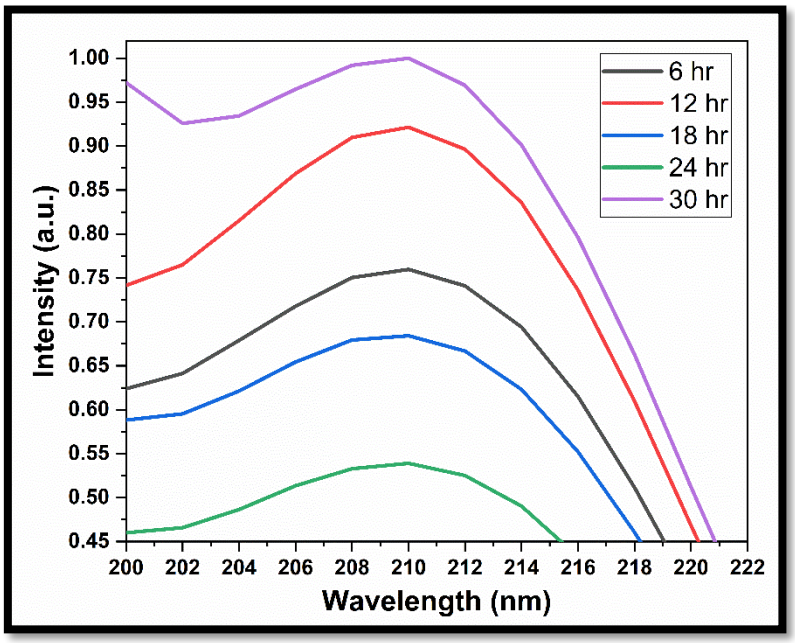

Fig. Uv-Vis absorption spectra of NGQDs.

λ_{onset} = 210nm from the above graph.

$E_g^{opt} = \frac{1240}{210} = 5.905$ eV.

The bandgap of NGQDs at 210 nm wavelength is 5.905 eV.

7.1.2 Photoluminescence (PL)

Photoluminescence (PL) happens when light energy or photons excite any substance, resulting in photon emission. The process is summarised as follows: light is focused onto a sample, where it is absorbed, and photo-excitation occurs. As a result of photo-excitation, the electron jumps to a higher energy state and subsequently relaxes to a lower energy state, releasing energy as photons. The light emitted as a result of this process is known as photoluminescence (PL). PL can be used to measure band gap, impurity levels and defect detection, recombination mechanism, material quality, and molecular structure and crystallinity.

For the intensity measurement using PL of NGQDs and GQDs 3ml samples each are taken in all the scenarios.

Fig(1a) shows the PL emission spectrum of NGQDs at excitation 330 nm, which clearly shows the intensity of NGQD30 is maximum and NGQD6 is minimum .

Fig(1b) shows PL emission spectrum of GQDs at excitation 330 nm, which clearly shows the intensity of GQD24 is maximum and NGQD6 is minimum .

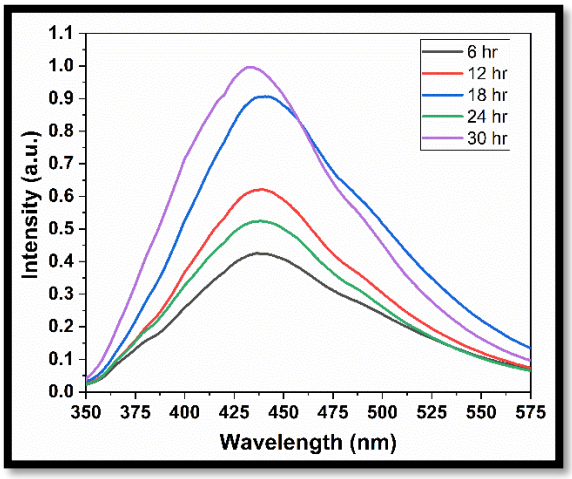

Fig. (1a) PL Emission spectra of NGQDs.

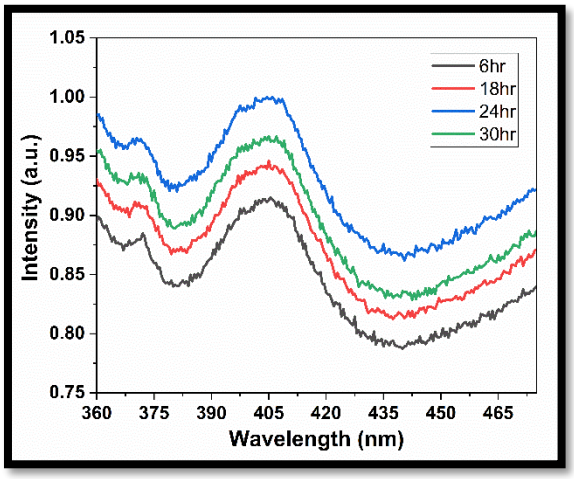

Fig. (1b) PL Emission spectra of GQDs.

Excitation variation: The excitation wavelength is varied to show whether Graphene Quantum Dots and Nitrogen-doped ones show excitation-dependent emission.

Fig(2a) shows the excitation dependent nature of NGQD24, 3ml sample is taken in each case for this purpose. Similarly, Fig(2b) shows the excitation dependent nature of GQD24.

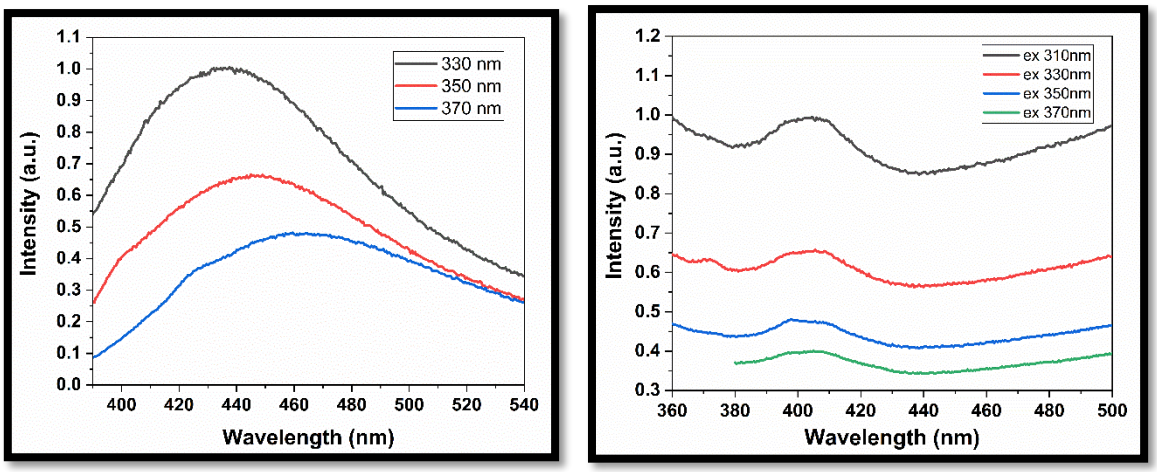

(2a) (2b)

Fig. (2a) Excitation-dependent nature of NGQD24. Fig. (2b) Excitation-dependent nature of GQD24.

Figures (2a) and (2b) indicate that as the excitation wavelength increases, the intensity drops. This is demonstrated by the fact that as excitation increases, the emission spectra of Graphene Quantum Dots and Nitrogen-doped Graphene Quantum Dots decreases.

Amino acid sensing: First, merely 3 ml of NGQD30 is consumed; for NGQD30(A1.0), NGQD30(C1.0), and NGQD30(G1.0), 2 ml of NGQD30 is taken, and 1 ml of Arginine, Cystine, and Glycine are added, respectively.

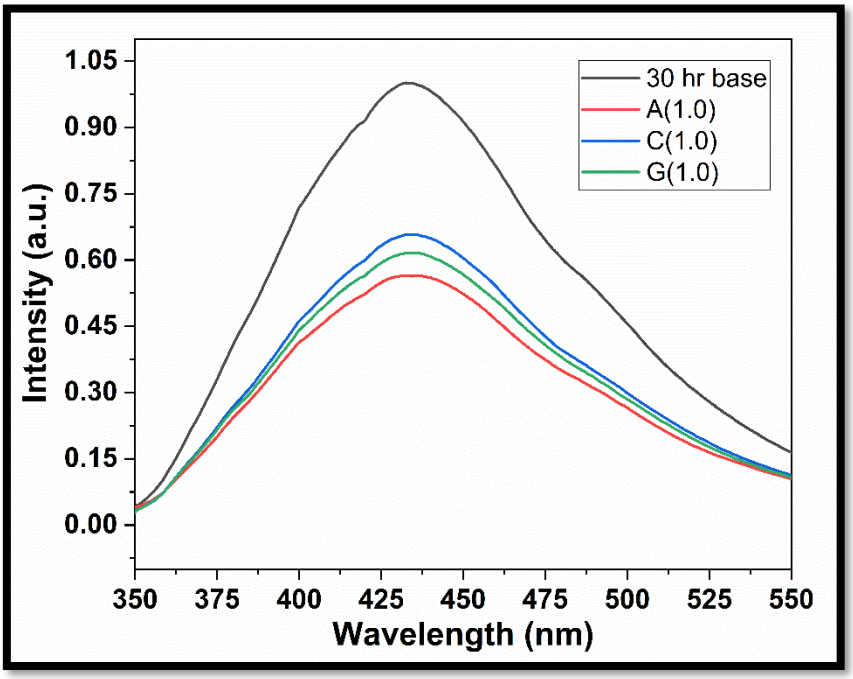

Fig. (3) shows intensity of NGQD30, NGQD30(A1.0), NGQD30(C1.0) & NGQD30(G1.0).

The NGQD30 sample is quenched with Arginine, Glycine and Cystine; Arginine shows the best result with sample NGQD30.
Intensity of NGQD30 > NGQD30(C1.0) > NGQD30(G1.0) > NGQD(A1.0)

Amino acid sensing using glutathione: At first a solution was made of Glutathione(G50), with 50 mg Glutathione in 10 ml De-ionized water. Nine solutions of NGQD18, De-ionized water, and Glutathione(G50) of varying concentrations are prepared in a total volume of 3 ml to analyse their behaviour utilising PL emission spectra.

Table. Concentrations of NGQD18, DI and Glutathione (G50).

Sample name	**Sample (ml) (NGQD18)**	**DI (ml)**	**Glutathione (ml) (G50)**
V1	2	1	--
V2	2	0.5	0.5
V3	2	0.4	0.6
V4	2	0.3	0.7
V5	2	0.2	0.8
V6	2	0.1	0.9
V7	2	--	1
V8	2	0.6	0.4
V9	2	0.7	0.3

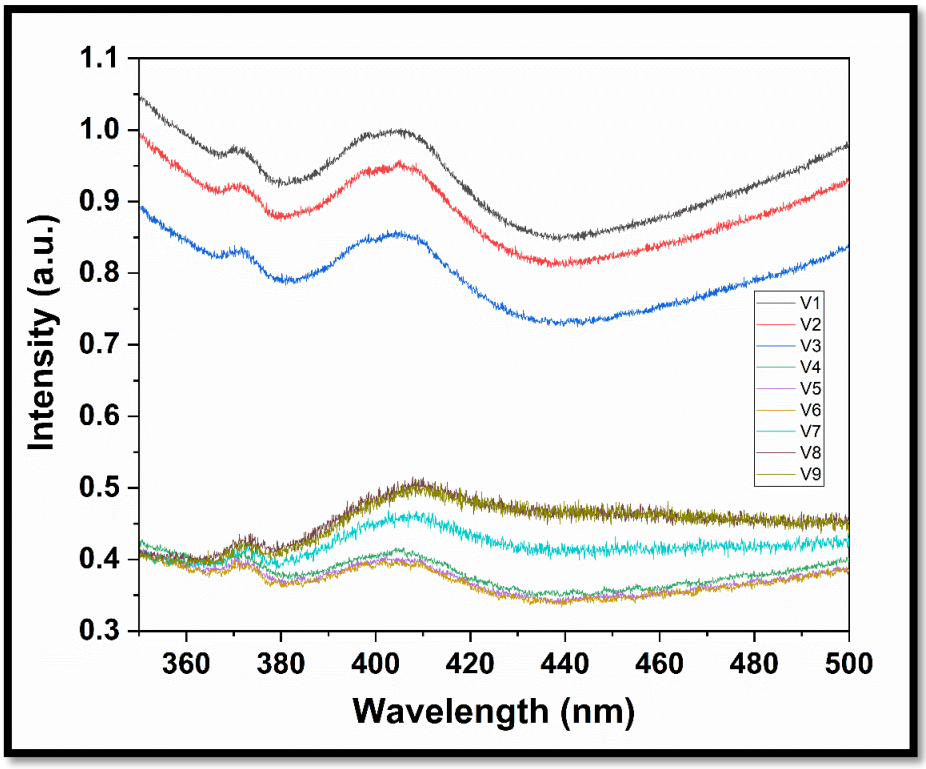

Fig. (4) Glutathione sensing using NGQD18.

Intensity: V1>V2>V3>V8>V9>V7>V4>V5>V6.

Glutathione sensing can be observed with Nitrogen-doped Quantum Dots that are prepared.

Metal Sensing: The Fe solution was produced with 10mg $FeCl_3$ in 10ml DI. In a total volume of 3 ml, fourteen solutions of NGQD30, De-ionized water, and Fe solution of different concentrations are created to analyse their behaviour using PL emission spectra.

Table. Concentrations of NGQD30, DI and Fe solution.

Sample name	**Sample (ml) NGQD30**	**DI (ml)**	**Fe sol^{n}**
NGQD30	3	--	--
Fe1	2	--	1
Fe0.5	2	0.5	0.5
Fe0.2	2	0.8	0.2
Fe0.15	2	0.85	0.15
Fe0.11	2	0.89	0.11
Fe0.1	2	0.9	0.1
Fe0.05	2	0.95	0.05
Fe0.04	2	0.96	0.04
Fe0.03	2	0.97	0.03
Fe0.02	2	0.98	0.02
Fe0.01	2	0.99	0.01
Fe0.005	2	0.995	0.005
Fe0.001	2	0.999	0.001

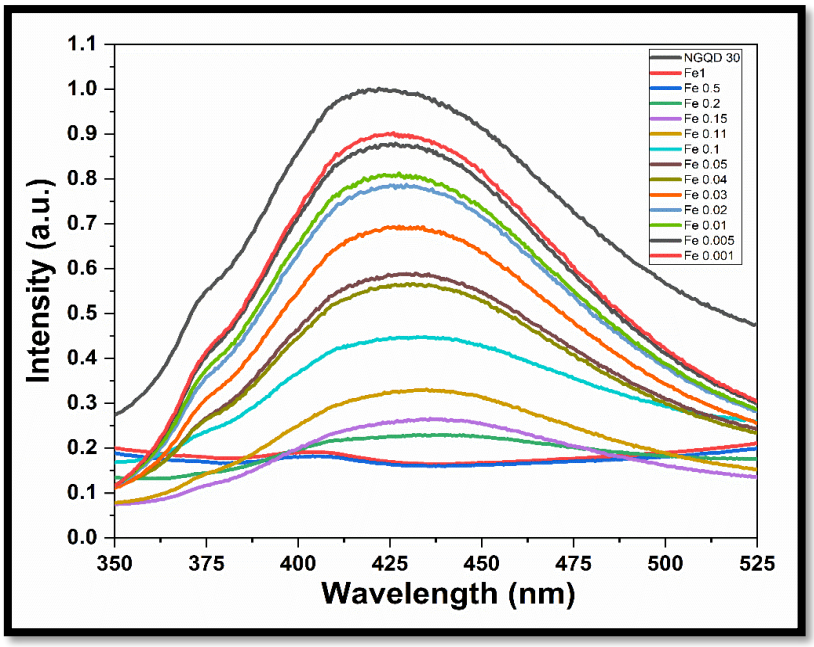

Fig. (5) Metal sensing with Fe in NGQD30.

Thus, metal sensing was observed with Nitrogen-doped Graphene Quantum Dots.

7.2 Structural Analysis

High-resolution transmission electron microscopy (HRTEM) and X-ray photoelectron spectroscopy were used for structural and compositional studies (XPS).

7.2.1 HRTEM

The length and orientation of the GQD and NGQD layers can be easily expressed using HRTEM image processing technologies. HRTEM is a legitimate diffraction device that may be used to directly observe the morphological properties of a substance while also getting a great amount of microcrystalline structure information [4].

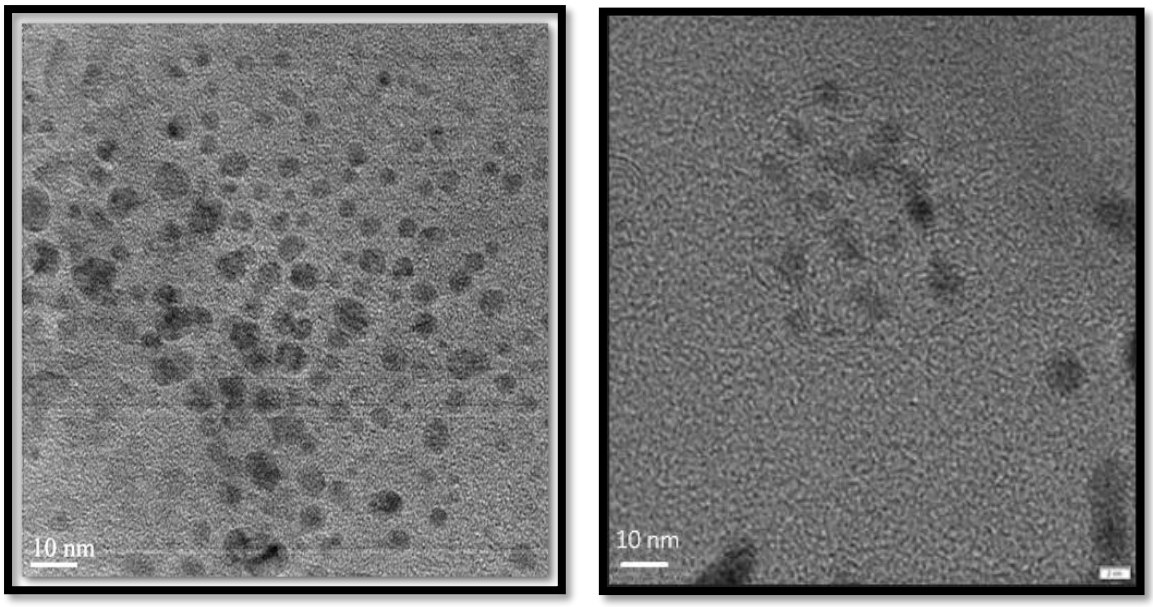

(6a) (6b)

Fig. (6a) HRTEM image of GQD24. Fig. (6b) HRTEM image of NGQD24.

7.2.2 XPS analysis

X-ray photoelectron spectroscopy (XPS) analysis shows the composition of as-synthesized C-QDs. Nitrogen was found in the C-QDs from the XPS spectrum as shown in Figure. The high-resolution spectra of N1s revealed the presence of both pyridinic (394.8 eV) and pyrrolic (398.2 eV) N atoms. Apart from that the presence of Amine (394.1 eV) and Graphitic (396.4 eV) components can also be seen, illustrating that the C-QDs were successfully doped with nitrogen atoms.

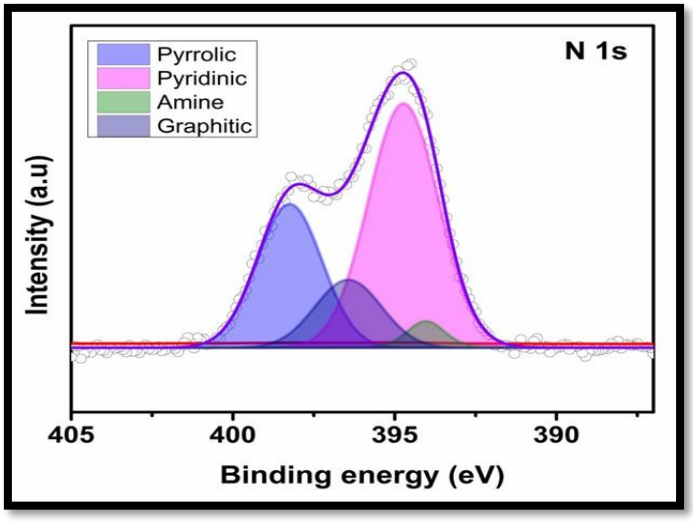

Fig. (7) Fig. XPS spectrum of GQDs (High-resolution spectra XPS of N1s)

Reference

1. S. Zhu, Y. Song, J. Wang, H. Wan, Y. Zhang, Y. Ninga and B. Yang, Photoluminescence mechanism in graphene quantum dots: Quantum confinement effect and surface/edge state, Nano Today, 2017, 13, 10–14.
2. L. Tang, R. Ji, X. Li, K. S. Teng and S. P. Lau, Size-dependent structural and optical characteristics of glucose-derived graphene quantum dots, Part. Part. Syst. Charact., 2013, 30, 523–531.
3. K. A. Ritter and J. W. Lyding, The influence of edge structure on the electronic properties of graphene quantum dots and nanoribbons, Nat. Mater., 2009, 8, 235–242.
4. HRTEM analysis of the aggregate structure and ultrafine microporous characteristics of Xinjiang Zhundong coal under heat treatment Xueping Li[1,2,3] & Qiang Zeng[1,2,3*]

Chapter 8

Conclusion

&

Scope for future works

8.1 Conclusion

Graphene Quantum Dots and Nitrogen-doped Graphene Quantum Dots were used in this study. Graphene Quantum Dots were successfully created using a low-cost hydrothermal synthesis procedure, and the products are being modified by adjusting the duration while the other parameters remain constant. Uv-Vis Spectroscopy was used to compute the bandgap of the Nitrogen-doped Graphene Quantum Dots. Using PL analysis, we can see the excitation-dependent emission spectra of Graphene Quantum Dots and Nitrogen-doped Graphene Quantum Dots.

The Nitrogen-doped Graphene Quantum performs well for metal detection and amino acid sensing, as seen by their PL spectrum. Our sample could detect amino acids such as Arginine, Cystine, Glycine, and Glutathione, as well as metals such as Fe. Thus, using Graphene Quantum Dots, is a low-cost and accurate for detecting amino acids and metals.

8.2 Scope for future works

Graphene quantum dots (GQDs), a zero-dimensional (0D) nanomaterial of the carbon family, have shown promising biomedical applications due to their ultra-small size, non-toxicity, biocompatibility, excellent photostability, tunable fluorescence, and water solubility, among other properties, capturing considerable attention in the biomedical field.

Despite substantial advances and demonstrated amazing benefits, the prospective bioimaging applications of GQDs have not yet been fully explored due to several unresolved obstacles. GQD research is still in its early stages. As a result, while there is a large development space for GQDs, there are still some issues that need to be addressed, such as low product yield and quantum yield, deficiencies in accurately controlling lateral dimensions as well as surface chemistry, the perplexing PL mechanism, narrow spectral coverage, a lack of tailor-made control of optical properties, and so on. Because of the advancements in grapheme, CDs, and even semiconductor quantum dots, there are several applications in biology, electronics, and other fields.